ABSTRACT

RADIATION CHEMISTRY STUDIES OF WATER
AS RELATED TO THE INITIAL LINEAR ENERGY
TRANSFER OF 11-23 MEV PROTONS

by Gerald L. Kochanny, Jr.

Previous studies of the effect of initial linear energy transfer $(dE/dx)_i$ or LET_i, in the radiation chemistry of water have covered the LET_i region above 0.4 ev/Å. This report describes studies of the LET_i region from 0.2 to 0.4 ev/Å.

Ferrous sulfate, ceric sulfate and ceric + thallous sulfate dosimeters were irradiated with protons of specific energy in the range 11 to 23 Mev. Representative G values from the yields obtained for various proton energies are: $G(Fe^{+3})$ yields for 22.0, 18.0, 15.0 and 11.0 Mev protons are 12.64, 12.18, 11.75 and 11.29, respectively; $G(Ce^{+3})_{Tl}$ + yields for 22.0, 18.0, 15.0 and 11.0 Mev protons are 6.71, 6.46, 6.27, and 6.01, respectively; $G(Ce^{+3})$ yields for 22.0, 18.0, 15.0 and 11.0 Mev protons are constant at 2.95. From these results, G values for H, OH, H_2, H_2O_2 as well as G_{-H_2O} were calculated. Experimentally determined and calculated G values, smoothly extend the earlier data.

The work entailed accurate proton beam current and energy measurements for which methods had to be devised. The integrated area under the elastic peak of the energy spectrum of protons scattered by a very thin nickel foil, as recorded by a scintilla-

tion counter, was related to the proton beam current absorbed by the sample. Proton beam energies were determined by evaluating the mean range of protons in aluminum. Protons were degraded to approximately 6 Mev. The exact range was determined from the amount of ferrous ion oxidation effected in a ferrous sulfate dosimeter and the amount of absorber used to degrade the proton beam energy.

RADIATION CHEMISTRY STUDIES OF WATER AS RELATED TO THE INITIAL LINEAR ENERGY TRANSFER OF 11-23 MEV PROTONS

By

Gerald L. Kochanny, Jr.

A THESIS

Submitted to
Michigan State University
in partial fulfillment of the requirements
for the degree of

DOCTOR OF PHILOSOPHY

Department of Chemistry

1962

ACKNOWLEDGMENTS

The author gratefully acknowledges the sincere interest and guidance of Dr. Andrew Timnick, his major professor, from Michigan State University, and of Dr. C. J. Hochanadel of the Chemistry Division and Dr. C. D. Goodman of the Electronuclear Research Division at the Oak Ridge National Laboratory, who served as research advisors and members of his special committee at the Laboratory. He also thanks the Oak Ridge Institute of Nuclear Studies for sponsoring this research under the Oak Ridge Graduate Fellowship Program.

In addition, the author wishes to express his gratitude to the following; H. A. Mahlman, J. F. Riley, and J. W. Boyle of the Chemistry Division for their many hours of valuable consultation, to C. B. Fulmer and J. B. Ball of the Electronuclear Research Division who also gave generous amounts of their time in consultation and who suggested the current measuring technique used in this investigation and to E. L. Olsen who contributed his ingenuity in electronics to the project. Thanks are due also to Fred Burnette who constructed all of the mechanical apparatus used in the cyclotron bombardments, and to Miss Jeanette Hamby who typed the manuscript for this work.

A special debt of gratitude is due the author's wife, Janet Lenore, for her patience, kindness and understanding throughout the course of this study.

VITA

Gerald L. Kochanny, Jr. was born in Bay City, Michigan on August 25, 1933. He received his elementary education at St. Stanislaus Elementary School and graduated from St. Joseph High School in June of 1951. He was awarded a Bachelor of Science in Chemistry degree from the University of Michigan in June 1955 and the Master of Science degree in Organic Chemistry from Bradley University in Peoria, Illinois in June 1958. He received a Regents-Alumni Scholarship for three years at the University of Michigan and served as a graduate teaching assistant in General and Organic Chemistry at Bradley University. He began his studies for the Doctor of Philosophy degree at Michigan State University in September 1957, and there held a graduate teaching assistantship in General and Analytical Chemistry for two and one-half years. His research for the doctoral dissertation was performed in the Electronuclear Research Division and the Chemistry Division of the Oak Ridge National Laboratory under the sponsorship of the Oak Ridge Institute of Nuclear Studies.

Mr. Kochanny is a member of Sigma Xi and the American Chemical Society.

TABLE OF CONTENTS

LIST OF TABLES

page

LIST OF FIGURES

I. INTRODUCTION

Radiation chemistry is the study of the chemical action of all types of high-energy or ionizing radiations.

Radiation induced decomposition of water has been studied extensively with various kinds of radiation. Yields of various species formed during the decomposition of water have been evaluated for ionizing radiations as related to their linear energy transfer, LET. Linear energy transfer, or stopping power, is defined as the rate of energy loss in a material per unit distance travelled by a particle of radiation. Recent reviews[5,18] point out the lack of experimental data in the 0.02 to 0.4 ev/Å LET region, with the exception of data accumulated from cobalt-60 gamma rays. Most experiments conducted in this region have been done with x-rays, for which dosimetry is, at best, difficult. Recently, however, there has been a greater application of cyclotron-produced radiations. At present, the cyclotron is a convenient source of radiation in the 0.2 to 5.0 ev/Å LET region.[2,3,8-11,17]

This work was undertaken to obtain radiolytic oxidation and reduction yields in the 0.2 to 0.4 ev/Å region for three different aqueous solutions, from which the calculation of G_{H_2}, $G_{H_2O_2}$, G_H, G_{OH} and G_{-H_2O} can be made. Such values are useful for the purpose of testing proposed theories on the chemical action of radiation. Systems selected for this study were:

(1) acidified, aerated ferrous sulfate solutions,

(2) acidified, aerated ceric sulfate solutions, and

(3) acidified, aerated ceric sulfate solutions with added thallous sulfate.

The source of radiation for this work was the Oak Ridge 86-inch cyclotron, which has a base proton beam energy of 23 Mev. Lower energy protons were obtained by attenuation of the proton beam with aluminum absorbers.

II. HISTORICAL

The study of the chemical effects of ionizing radiation began in the middle of the nineteenth century with the discovery of chemical transformations occurring during electrical discharges in gases. Actually, chemical changes produced by electrical discharges in gases were observed in the eighteenth century. The first application of this phenomenon was made by von Siemens in 1857, when he invented a device for producing ozone from oxygen.

The early work in the field of radiation chemistry was motivated, to a large extent, by recognition that chemical transformations produced by electrical discharge can proceed against the thermodynamic potential, and thus provide a means of converting electrical energy into chemical free energy. This branch of radiation chemistry has never matured because of the extreme difficulty of making quantitative studies, especially of the number and character of initial ionizations. Recent developments in the understanding of electrical discharges offer promise of providing the needed quantitative basis for further experiments along this line.

Radiation chemistry emerged as a legitimate science early in the twentieth century when the availability of x-rays and radiations from radioactive sources influenced the attainment of accurate dosimetry. The discovery of radiation sources, and early experiments with them, by scientists such as Becquerel, the Curies and Soddy led to this branch of chemistry.

Research on the radiation chemistry of water began about 1900 with the discovery that H_2, H_2O_2 and O_2 are produced upon irradiation of water and aqueous solutions. At about the same time, studies of gaseous systems intensified. The approximate equality of the number of ions produced and the number of molecules transformed, in a majority of cases, was observed. Interpretations of experimental results were often based on the theory of photochemistry, although the primary processes of radiation chemistry are considerably more complicated than those of photochemistry. In these early stages of research in radiation chemistry, the most prominent names were Lind, Mund and Fricke. Lind and Mund are recognized individually for their research on gaseous systems, using α-particle sources. Fricke is known for his work with aqueous systems, and especially for the application of them to x-ray dosimetry.

Present day studies in radiation chemistry involve the detailed identification and analysis of radiolytic products and studies of the kinetics and mechanisms of various radiation induced reactions.

III. THEORY

The several, readily available review articles,[21-42] and especially the most recent complete compendia,[5,18,43] on the subject of radiation chemistry, may be consulted for a complete survey of this topic. In this report, only a brief summary of the facts and theories which have a direct bearing on this investigation, and which lend something to the continuity and completeness of the report will be given in the following paragraphs of this section.

Characteristic Effects of Ionizing Radiation in Liquid Water. Ionizing radiation may be defined as any type of electromagnetic radiation or charged particle which causes ionization upon passage through, or absorption by, matter. The more familiar ionizing radiations are γ-rays, x-rays, electrons, α-particles, deuterons and protons.

Although pure, air-free water is decomposed very slightly on irradiation with γ-rays or x-rays, the net decomposition is increased by use of heavier, more densely ionizing particles, and is appreciably greater in the presence of organic and inorganic solutes. The observable products in pure water are H_2, H_2O_2 and O_2. In the presence of a reactive solute one observes H_2, and an oxidized or reduced product. Oxygen is observed if H_2O_2 reacts as a reducing agent. These observations, and most other data on water radiolysis can be explained by assuming initial decomposition of water to

hydrogen atoms and hydroxyl radicals (H and OH). Generally, the existence, properties and numbers of these radicals are inferred from the chemical reactions produced by their action on dissolved substances in water. However, direct experimental evidence for these radicals, obtained mainly from optical and mass spectrometry, does exist. Paramagnetic resonance absorption experiments have demonstrated the existence of hydrogen atoms in ice irradiated with electrons.[44] Absorption spectrometry has yielded evidence for the existence of hydroxyl radicals, by the characteristic absorption of this radical at 3064 Å, in water decomposed by electric discharge[45] and by ionizing radiation,[46] to mention just a few of the studies in this area.

Processes occurring during the passage of ionizing radiation through an aqueous solution are summarized in equation (1). (See reference 18, p. 154).

$$(1) \qquad H_2O \xrightarrow{10^{-18} \text{ to } 10^{-15} \text{ sec.}} H_2O^+, H_2O^* \xrightarrow{\sim 10^{-12} \text{sec}} H, OH$$

$$\xrightarrow{\sim 10^{-8} \text{ to } 10^{-7} \text{ sec.}} H_2, H_2O_2, H_2O, OH, H \longrightarrow \text{(reactions with solute)}$$

Times indicated in this equation are obtained from calculations based on reaction rate studies and are approximate values for a one Mev electron passing through water. They would not be appreciably different for 11-23 Mev protons, used in this study. The most important probable reactions occurring on passage of ionizing radiation through

water[18] are expressed in equations (2-6). They illustrate the

(2) $H_2O \rightsquigarrow H_2O^+, H_2O^*, \quad {}^{H}\!\diagdown\!O - H \text{-----} {}^{+}O\!\diagup\!{}^{H}_{H}$, electrons

(3) $H_2O^* \longrightarrow OH + H + \sim 2$ ev kinetic energy

(4) ${}^{H}\!\diagdown\!O - H \text{-----} {}^{+}O\!\diagup\!{}^{H}_{H} + e^- \longrightarrow H_3O^+ + OH + e^-$

(5) $H_2O^+ + e^- \longrightarrow H_2O^* \longrightarrow OH + H +$ kinetic energy

(6) $H_2O + e^-_{aq.} \longrightarrow H + OH^-_{aq.}$

formation of reactive H and OH radicals and are consistent with mass spectrometry data.

The path of an ionizing particle through water is given complete coverage in the above-mentioned review articles. Briefly, the situation may be described in terms of the two extreme types of ionizing particles:

(1) The light, high speed, charged particles, which move through water leaving a sparsely ionized track and,

(2) the heavy, slower moving, charged particles which produce a densely ionized track.

Examples of the first type are high speed electrons which pass through water producing ionizations several thousand angstroms apart, while an example of the second type is a low energy α-particle which produces an essentially continuous ionization track resulting from overlapping zones of ionization. Gamma and x-rays

have a low LET (~ 0.02 ev/Å) whereas a low energy α-particle has a high LET (~ 10 ev/Å for a 3.5 Mev α-particle).

The mechanism for the dissipation of the energy of an incident particle is essentially the same for all types of radiation. Current thinking on this matter has been expressed by Magee[47] and Platzman.[48] As an ionizing particle passes through water, spacing of the primary ionizations is dependent on the LET of the particle. Generally, more electronic excitations than ionizations are produced. A large majority of the secondary electrons ejected in the ionization acts have an energy of less than 5 ev, although energy distribution over an energy spectrum up to a few thousand electron volts does occur. The more energetic electrons are capable of causing little regions of high ionization and excitation since the path of the secondary electron is frequently deviated by collisions thereby confining its action to a small volume. These regions of high excitation and ionization are commonly referred to as spurs. The secondary electrons are estimated to have an average energy of approximately 75 ev, which is dissipated in a volume element having a diameter of about 20 Å, in which approximately five water molecules are dissociated. In the course of its degradation to about 6.5 ev (the lowest excitation potential of water), a 75 ev electron makes about ten collisions, during an interval of 10^{-15} seconds, while travelling about 30 Å. Those electrons with energy below the lowest excitation potential of water lose their energy by

dipolar interaction and molecular vibrational excitation. These sub-excitation electrons lose energy down to about 0.025 ev (are thermalized) in about 10^{-13} seconds, during which time they have travelled a distance of about 20 Å, from the positive ion but a total distance of about 1000 Å due to many large angle deflections. The positive parent ion then draws the electron back with its now sufficient coulomb field, thus yielding a highly excited water molecule which dissociates to H and OH. The kinetic energy received by the H atom in this process is sufficient to move it a few molecular diameters from the OH radical before it is thermalized. The spurs, which vary in size and spacing are relatively widely separated for fast primary particles and overlap for slow particles. In the latter case, they form a cylindrical region of high ionization and excitation approximately 20 Å in diameter. Between these extremes of the track structure, a compromise between the isolated sphere and the cylindrical model is operative.

Those relatively few secondary electrons which have an energy of several hundred or more electron volts, produce a true track of their own, which branches off from the primary track. This track is referred to as a delta ray.

Most of the reactive intermediates are produced in the spurs. This leads to the conclusion that the concentration of reactive intermediates in the system is non-homogeneous, and thus time-

dependent. Therefore, subsequent reactions of intermediates are diffusion controlled. On this basis, a diffusion model of the events occurring during the radiolysis of water has been proposed, and is related to experimental data by the diffusion kinetics theory.

Reaction Yields from the Radiolysis of Water. Reaction yields produced by radiation are expressed in terms of the number of molecules, ions, or radicals converted per 100 ev of energy absorbed, and are denoted by the letter G. In this manuscript, an experimentally observed yield is denoted by G with the formula of the substance in parenthesis (e.g., $G(H_2)$). The yields of substances formed initially from water are denoted by G, with the formula of the substance as a subscript (e.g., $G_{H_2O_2}$). Thus, $G(H_2O_2)$ refers to the actual amount of hydrogen peroxide produced upon radiolysis, as determined by chemical analysis, while $G_{H_2O_2}$ is a derived quantity and refers to the amount of hydrogen peroxide which would be produced directly from water by radiation.

The four most important products from water radiolysis are H, OH, H_2, and H_2O_2, and their yields are related by the equation of material balance:

$$(7)\quad G_{-H_2O} = G_H + 2G_{H_2} = G_{OH} + 2G_{H_2O_2}$$

Linear Energy Transfer. Energy lost by a charged particle through ionization or excitation of any material depends on the

velocity and the magnitude of the charge of the particle. Since a proton is 1836 times heavier than an electron, a 1 Mev electron will travel $(1836)^{1/2}$ or 42.8 times faster than a 1 Mev proton. A convenient, often used, parameter for characterizing radiation is the amount of energy lost per unit distance travelled, usually denoted by -dE/dx, often called linear energy transfer or stopping power. For ions at non-relativistic velocities, it is expressed by equation (8),[49] where m and e are the electron mass and charge,

$$(8) \quad -\frac{dE}{dx} = (2\, e^4 z^2 \frac{NZ}{E}) (\frac{M}{m}) \ln (\frac{4E}{I}) (\frac{m}{M})$$

M and E are the mass and energy of the moving charged particle, z is the number of unit charges carried by the particle, NZ the number of electrons per unit volume of irradiated material, and I is a parameter characteristic of each material, sometimes called the stopping potential. The best value of I for water is 66 ev, according to Schuler and Allen.[2] Equation (8) reduces to equation (9) for protons, where E is in Mev and -dE/dx is in ev/Å.

$$(9) \quad -\frac{dE}{dx} = \frac{1.870}{E} \log_{10} \frac{E}{0.0605}$$

Special attention should be drawn to the fact that, as a particle of radiation traverses matter it loses energy, hence, its LET is constantly changing. LET values calculated from equations (8) and (9) and plotted in the figures of this report are initial LET, LET_i. Figure 1, which was calculated from

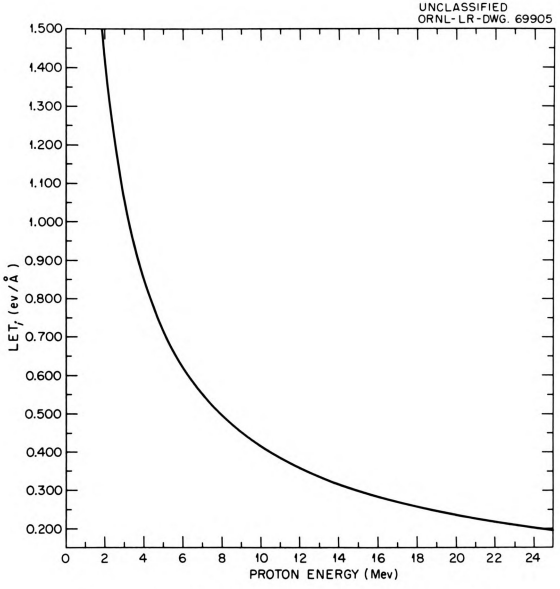

Figure 1. Linear Energy Transfer for Protons in Water.

equation (9), illustrates how LET_i changes as a function of proton energy.

The immediate effects of LET variation were described in the previous discussion of track variation. It was pointed out, that for low LET, the track may be described as a series of isolated spheres, while for large LET, the spheres overlap to form a cylindrical volume element. The result of this effect is, that in the case of low LET, there is much less recombination of radicals to produce water, H_2, and H_2O_2. Thus, the radical yields are much higher than the molecular yields. For increasing LET, due to the proximity of the radicals, the radical yields decrease and the molecular yields increase. At high LET, the radical yields approach zero, indicating nearly complete radical recombination. Also at high LET, the observable water decomposition decreases (greater reformation of water) while the gross water decomposition increases.

Stoichiometric Relations in the Radiolysis of Water and Aqueous Solutions. a. Pure Water. Irradiation of very pure, degassed water, in a sealed ampoule, using γ-rays or x-rays, produces an almost undetectable decomposition of the water. Decomposition does occur, but in the absence of scavengers, the radicals produced react with the molecular products producing a very low steady state concentration of H_2, H_2O_2 and O_2. The events occurring during the radiolysis of pure water are depicted in equations (2-6) and (10-18).

(10) $H + H \longrightarrow H_2$

(11) $OH + OH \longrightarrow H_2O_2$

(12) $H + OH \longrightarrow H_2O$

(13) $H_2 + OH \longrightarrow H_2O + H$

(14) $H_2O_2 + OH \longrightarrow H_2O + HO_2$

(15) $H_2O_2 + H \longrightarrow H_2O + OH$

(16) $O_2 + H \longrightarrow HO_2$

(17) $HO_2 + HO_2 \longrightarrow H_2O_2 + O_2$

(18) $HO_2 + OH \longrightarrow H_2O + O_2$

Initially, H_2 and H_2O_2 are produced according to equations (10) and (11). The interaction of these molecular products, equations (13-18), with H and OH radicals which were produced according to equations (2-6), leads to a steady state concentration of H_2, H_2O_2 and O_2. The steady state concentration is increased by an increase in dose rate or LET. With a large dose rate it is possible for the intermediates from spurs in adjacent tracks to react. The steady state concentration has been observed to increase up to 10 ev/Å, beyond which no experimental data are available.

b. Aerated, Acidified Ferrous Sulfate Solutions. The presence of a reactive solute causes a drastic change in the net decomposition of water. A solute capable of reacting with H and OH radicals prevents the attainment of a steady state concentration of H_2,

H_2O_2 and O_2. Molecular and radical yields may be deduced from results obtained by direct quantitative analysis of molecular products and/or analysis of scavenger products. Solutes which react by simple mechanisms are preferred for this kind of study. Ferrous sulfate solutions have been studied extensively in radiation chemistry, and the processes contributing to the overall reaction are well understood. Generally, solutions used in these studies are prepared 0.001 M in ferrous sulfate, 0.001 M in sodium chloride and 0.4 M in sulfuric acid. The predominant reactions occurring upon radiolysis of this solution are represented by equations (16) and (19-22). The total observed oxidation yield

(19) $Fe^{+2} + OH \rightarrow Fe^{+3} + OH^-$

(20) $Fe^{+2} + HO_2 \rightarrow Fe^{+3} + HO_2^-$

(21) $H^+ + HO_2^- \rightarrow H_2O_2$

(22) $Fe^{+2} + H_2O_2 \rightarrow Fe^{+3} + OH^- + OH$

is represented by equation (23). In the absence of oxygen,

(23) $G(Fe^{+3}) = 2G_{H_2O_2} + 3G_H + G_{OH}$

equations (16) and (20) are replaced by equation (24), giving

(24) $Fe^{+2} + H_2O + H \rightarrow Fe^{+3} + OH^- + H_2$

a total yield expressed in equation (25). These mechanisms for

(25) $G(Fe^{+3})_{-O_2} = 2G_{H_2O_2} + G_H + G_{OH}$

the decomposition of ferrous sulfate are generally accepted, and investigations such as the present one make use of them in the calculation of molecular and free radical yields. As mentioned above, ferrous sulfate solutions used in radiation chemistry, are generally prepared 0.001 M in sodium chloride. This is done to avoid the difficulties which arise in the presence of organic impurities. The effect of these impurities is to decrease the yield of iron oxidized in deaerated solution and to increase it in aerated solution. This effect is best explained as a reaction of OH radicals with organic molecules as described in equation (26).

(26) $OH + RH \rightarrow H_2O + R$

In deaerated solution, the organic radicals generally reduce ferric ions rather than oxidize ferrous ions. In aerated solution, an RO_2 type radical may be produced which can either hydrolyze to HO_2 or react with ferrous ions to form ferric ions and hydrogen peroxide. Thus, an OH radical which can oxidize one ferrous ion is converted to a radical which can oxidize three ferrous ions. The effect of these impurities is eliminated by preparing the solution 0.001 M in chloride ions. Chloride ions react with OH according to equation (27), and the resulting Cl atoms react more

(27) $OH + Cl^- + H^+ \rightarrow H_2O + Cl$

rapidly with ferrous ions than they do with the organic impurities.

Besides its use in studies of mechanisms of radiation induced water decomposition, the ferrous system is an excellent dosimeter, and is extensively used in this capacity.

c. Aerated, Acidified Ceric Sulfate Solutions. In contrast to ferrous sulfate solutions, the net effect of the radiolysis of ceric sulfate solutions is a reduction. Ceric ions are reduced by H, HO_2 and H_2O_2 according to equations (28-30), and the product

(28) $Ce^{+4} + H \rightarrow Ce^{+3} + H^+$

(29) $Ce^{+4} + HO_2 \rightarrow Ce^{+3} + H^+ + O_2$

(30) $Ce^{+4} + H_2O_2 \rightarrow Ce^{+3} + H^+ + HO_2$

cerous ions are oxidized by OH radicals as in equation (31). The

(31) $Ce^{+3} + OH \rightarrow Ce^{+4} + OH^-$

overall yield is expressed by equation (32). Solutions of ceric

(32) $G(Ce^{+3}) = 2G_{H_2O_2} + G_H - G_{OH}$

sulfate prepared for radiolysis are usually 0.0004 M in ceric ion and 0.4 M in sulfuric acid. The preparation of this solution is more elaborate than that of the ferrous sulfate solution, and is described in the Experimental section.

d. Aerated, Acidified Ceric Sulfate Solutions with Thallous Ion Added. The radiolytic reduction yield for this solution is numerically equal to the radiolytic oxidation yield for deaerated

ferrous sulfate solutions. The mechanism for this system was first explained by Sworski,[52] and is represented by equations (28-30) and (33-34). Thallous ion does not react spontaneously

(33) $Tl^{+} + OH \rightarrow Tl^{+2} + OH^{-}$

(34) $Tl^{+2} + Ce^{+4} \rightarrow Tl^{+3} + Ce^{+3}$

with ceric ion but successfully competes with cerous ion for the OH radical. Thus, OH oxidizes the thallous ion to the unstable divalent state which is immediately oxidized to the stable trivalent state by a ceric ion. The overall effect is the reduction of one ceric ion by one OH radical, as indicated in equation (35).

(35) $G(Ce^{+3})_{Tl^{+}} = 2G_{H_2O_2} + G_H + G_{OH}$

Ceric-thallous solutions used in radiolysis studies are prepared in a manner similar to that for ceric sulfate solutions, except the solution is made approximately 0.001 M in thallous ion.

Molecular and Free Radical Yields and Dosimetry. From the experimentally determined radiolytic yields, the equations for the overall oxidation and reduction yields, and the equation for material balance, one can calculate the corresponding molecular and free radical yields for specified conditions. The functions for radiolytic water decomposition yields are summarized as follows:

(23) $G(Fe^{+3}) = 2G_{H_2O_2} + 3G_H + G_{OH}$

(32) $G(Ce^{+3}) = 2G_{H_2O_2} + G_H - G_{OH}$

(35) $G(Ce^{+3})_{Tl^+} = 2G_{H_2O_2} + G_H + G_{OH}$

(7) $G_{-H_2O} = G_H + 2G_{H_2} = G_{OH} + 2G_{H_2O_2}$

From these four functions, involving three measurements, separate values for G_H, G_{OH}, $G_{H_2O_2}$, G_{H_2}, and G_{-H_2O} may be obtained. Although this investigation has examined only the effect of LET on the various yields, the effect of solute concentration, pH, and temperature can be determined in an analogous manner. The yields obtained from this study may be used in support of the more simple theories which were put forth in the previous paragraphs. Also, they may be used to test proposed models, such as the diffusion model, in an effort to arrive at a satisfactory one to explain the events which occur during the radiolytic decomposition of water. The most satisfactory theory to date, the diffusion kinetics theory, while generally considered to be qualitatively correct is still in its very early stages of development on a quantitative basis. This situation is due, primarily, to the complexity of the system, and the large number of unknown variables which must be considered.

On the other hand, accurately determined radiolytic yields are of immediate practical value to other investigators for dosimetry. If the energy or LET of a particular radiation is

known, the dose rate to a dosimeter solution may be determined from the amount of chemical conversion, and the G value of the dosimeter. Then, the dose rate to other samples, irradiated under identical conditions, may be determined by exposing them to radiation for a similar amount of time or some other easily standardized variable. A more subtle use of these values is the determination of the energy of the radiation, as described in the Experimental section.

Diffusion Kinetics Theory. The first theory of diffusion kinetics was developed by Jaffe[57,58] in an effort to explain the current flow between charged plates at a high potential which occur in gases upon irradiation. The theory was improved by Lea,[56,59-61] and developed more extensively by Magee and co-workers.[55,62,63] An excellent and complete compendium on the historical developments and the present day status of the diffusion kinetics theory has been written by Kuppermann.[64] A brief survey, according to Kuppermann, of those facets of diffusion kinetics which pertain to the results of the present investigation follows.

a. General Mathematical Formulation of the Diffusion Kinetics Model. The following assumptions are implicit in the diffusion kinetics model of radiation chemistry:

(1) The primary species, formed upon irradiation, are in thermal equilibrium with the surroundings before any chemical reaction occurs. At this stage, they are in a specific inhomogeneous spatial distribution depend-

ing on the type and energy of the incident radiation.

(2) The primary species proceed to diffuse according to macroscopic diffusion laws, and react with one another or with other species in the system.

(3) The reaction products of the primary species may be reactive and participate in further reactions.

(4) All reactions are assumed to follow rate laws similar to those obeyed by reactive species which are distributed homogeneously.

(5) The end-result is the formation of stable chemical products.

For sufficiently low density of absorbed energy, (low radiation dose rate) the chemical effects produced on irradiation of a system can be illustrated as a sum of the separate effects of individual particles. Conditions defined in this manner provide for the lack of dose rate effects, thus, the events along a single particle track may be considered as representative of the overall effects of radiation on a system. For this situation, the change of probability density C_i* at position P with respect to time, is the sum of the

*The diffusion and reaction-rate laws of macroscopic systems are usually expressed in terms of concentrations of the species involved. For a macroscopic system, containing a large number of particles, these concentrations, which are statistical averages of number densities over the whole or part of the system, represent a good approximation of the distribution of particles in the system. In considering track effects, however, due to the spatial inhomogeniety of the radical distribution, only a very small portion of the system, such as a track or a spur, is considered. In this case, diffusion and reaction-rate laws are expressed in terms of probability densities, and the number densities instead of being averaged over a large volume, as in the case of ordinary concentration, can be averaged over a large number of spurs or tracks.

effects of the net rate of diffusion of particles X_i to position P, and the rate of appearance and disappearance of these particles is due to chemical reactions occurring at P. Assuming that all of these reactions are either first or second-order, the corresponding representative equation is

$$(36)\quad \frac{\partial C_i(r,t)}{\partial t} = D_i \nabla^2 C_i - k_i C_i - \sum_j k_{ij} C_i C_j + \sum_e \bar{k}_e C_e + \sum_{m,n} \bar{k}_{m,n} C_m C_n$$

In this equation, D_i is the diffusion coefficient of species X_i, ∇^2 is the three-dimensional Laplacian operator, k_i is a rate constant for the first-order disappearance of X_i, k_{ij} is a second-order rate constant for the disappearance of X_i by reaction with X_j, $\bar{k}_e$ is a first-order rate constant for the appearance of X_i from X_e, and $\bar{k}_{m,n}$ is a second-order rate constant for the appearance of X_i by reaction of X_m with X_n.[64]

The number of equations (36) required for any system is equal to the number of different diffusing species X_i. In the case of the ferrous sulfate solutions used in this study, the different reactive species are OH, H, H_2O_2, H_2^+, Fe^{+2}, H^+ and H_2SO_5. For example, the diffusion kinetics equation for OH is

$$(37)\quad \frac{\partial [OH]}{\partial t} = D_{OH} \nabla^2 [OH] - k_{11} [OH]^2 - k_{19} [OH] [Fe^{+2}] + k_{22} [H_2O_2] [Fe^{+2}]$$
$$- k_{12} [H] [OH] - k_{13} [H_2] [OH] - k_{14} [H_2O_2] [OH] +$$
$$k_{15} [H_2O_2] [H] - k_{18} [HO_2] [OH]$$

In this equation, the subscripts of the k's refer to the corresponding equations of this report. Given the initial distributions $C_i(r,o)$ (i.e., the probability density of finding a particle of species X_i at point P = O + r at time t) equations such as (37) can, in principle, be integrated by numerical methods. Once the functions C(r,t) are known, the amounts of chemically stable products formed can be calculated. The accuracy of the calculation depends upon the accuracy with which the initial conditions can be defined. In defining these conditions the influence of such variables as LET, temperature, pH, phase, scavenger concentration and isotopic substitution upon the parameters of equation (36) or (37) must be considered.

A serious criticism of the diffusion kinetics model is that its representative equation contains so many unknown parameters that it can be adjusted to conform to any experiment by judicious selection of values for these parameters. However, in principle, most of these parameters are measurable, and since the development of the model, experimentalists have become increasingly aware of their importance in the interpretation of radiation chemistry. As the present state of experimental knowledge advances, these parameters will be measured, and applied to test the diffusion kinetics equations.

Another criticism to the model refers to the mathematical intractability of the diffusion kinetics equations. In view of the current development of high-speed computers, this criticism is rapidly becoming invalid.

Possibly the strongest reason for the acceptance of the diffusion kinetics model is that simplified modifications of it explain many experimental observations such as influence of LET and scavenger concentrations on radiolytic yields.

b. Comparison with Experiment. At the present stage of the diffusion kinetics theory, the most satisfactory theoretical treatment of the data from this report would accord with the treatment of Ganguly and Magee.[63] More advanced treatments of the theory are in existence, but the discussion of them is beyond the scope of this report.

The end result of the Ganguly and Magee treatment of the diffusion kinetics model is a plot of the fraction of radicals unscavenged (1-S) as a function of a quantity q. The latter is the product of $k_S C_S t_o$, where k_S is the rate constant for the radical scavenging reaction

(38) $R + S \longrightarrow$ Product

C_S is the concentration of scavenger solute, and t_o is a defined initial time, characteristic of the spur. This treatment involves the single radical theory in which water is considered a symmetrical two-radical compound R_2, and H_2, H_2O_2 and H_2O are the equivalent products of the recombination reaction

(39) $2R \longrightarrow R_2$.

By proper substitution of parameter values, suggested by the one-radical model, into equation (36), Ganguly and Magee[63] obtained an expression for the fraction of radicals scavenged S. From this expression, the theoretical plots of the fraction of radicals unscavenged (1-S) versus q, were prepared. The Ganguly and Magee equation is

$$S = \frac{k_S C_S t_o}{W_o} \int_1^\infty W_x dx \qquad (40)$$

or

$$\frac{dS}{dx} = q \frac{1}{\exp[q(x-1)]\left[1 + kW_o t_o \int_1^x \frac{\exp[-q(x'-1)]}{V_{x'}} dx'\right]}$$

where S, k_S, C_S, t_o and q are the same as previously defined, $x = t/t_o$, W_o is the total number of radicals in the track at time t_o, W_x is the total number of radicals in the track at time x, V is an expression directly related to the volume element of the spur, and is dependent on the nature of the track. It is through V, that the parameter S, the fraction of radicals scavenged, is related to the LET of the incident radiation, since the shape and size of the spur are functions of LET. Theoretical plots, for the one-radical diffusion model, of (1-S) versus log q are included in the Ganguly and Magee[63] paper, for 2.00, 7.68 and 10.00 Mev α-particles, 0.01, 0.05, 0.10 and 0.50 Mev β-particles, and for 0.1, 0.5, 1.0, 5.0 and 10.0 Mev protons.

The most direct method of comparing experimental data with theory, is to plot values for (1-S) which have been evaluated from experimental data, and those which have been calculated from theory, versus q, on the same graph. Although such a comparison is, in principle, simple, since (1-S) values are easily calculated (see Results and Discussion section and Table VIII), there is some difficulty in evaluting experimental q values, which are the products of k_S, C_S and t_o. The concentration of scavenger, C_S, is usually known, or can be measured, t_o was estimated by Ganguly and Magee to be 1.25×10^{-10} sec, but very few accurate values for k_S, the rate constant for the radical scavenging reaction, are known. Thus, it is not always possible to relate experimental q values to those calculated from theoretical considerations, unless values for k_S and t_o are known or measured. Also, in many instances, theoretically evaluated values for (1-S) are not available for comparison with experiment. For example, with respect to the present work, Ganguly and Magee plots are available for protons only up to 10 Mev. An extension of their calculations in a reasonable amount of time would require the use of a high-speed digital computer, and more information than is readily available, for the various parameters of equation (40). In view of these difficulties, the results obtained in the present study are not compared directly to the results which would be expected from the diffusion kinetic theory, rather they are

compared with the results of other investigations, which appear to be in accord with the diffusion kinetics model (see Results and Discussion section).

IV. EXPERIMENTAL

Reagents. This project involved the irradiation of three different chemical solutions: ferrous, ceric and ceric-thallous dosimeters.

The ferrous dosimeter was prepared 0.002 M in Baker and Adamson reagent grade ferrous ammonium sulfate, 0.001 M in Baker and Adamson reagent grade sodium chloride and 0.4 M in Baker and Adamson reagent grade sulfuric acid. Laboratory distilled water was used in the preparation of this solution since the results were found to be identical when more carefully purified water was used.

Since the ceric and ceric thallous dosimeters are particularly sensitive to impurities,[5] a more carefully designed procedure[1] was used in their preparation. G. Frederick Smith reagent grade ceric sulfate was heated in a stream of air at approximately 80°C for about one hour or until organic odors originally present were undetectable. A stock solution 0.004 M in ceric sulfate and 4 M in Baker and Adamson reagent grade sulfuric acid was prepared with the purified solid. The resulting solution was heated for approximately twelve hours at 100°C, and allowed to stand for several days before use.

Ceric dosimeter solutions were prepared from the stock solution by diluting with nine parts of water to one part of stock solution. The ceric-thallous dosimeter was prepared in the same manner, except that, after heating, the solution was made 0.002 M in A. D. Mackay purified thallous sulfate. The ceric and thallous sulfate dosimeter

undergoes rapid photochemical reduction on exposure to ordinary daylight. For this reason, the solution was stored in brown bottles, in a black bag. All measurements and irradiations were carried out in semi-darkness. Photochemical reduction under these conditions, was negligible. For the latter two dosimeters, water from a Barnstead still was purified by three successive distillations: (1) from an acid dichromate solution (2) from an alkaline permanganate solution and (3) finally in an all silica system. The purified water was stored in silica vessels.

To establish whether or not dosimeter solutions were properly prepared, a portion of each ceric and ceric-thallous dosimeter was irradiated in a cobalt-60 source at a dose rate of approximately 6×10^{16} ev ml^{-1} min^{-1} (see Table II) in a stoppered 1 cm. optical cell provided with non-coloring windows. The change in absorbance at 3200 Å produced by the radiolysis was followed with a Cary Model 11 MS recording spectrophotometer. The change in ceric ion concentration was calculated from the change in absorbance using 5609 liters $moles^{-1}$ $cm.^{-1}$ as the molar absorptivity.[1] The dose rate of the source had been previously determined from the rate of oxidation of the ferrous sulfate dosimeter using, for the pertinent calculations, 15.6 molecules of ferrous ions oxidized per 100 electron volts absorbed, and 2240 liters $mole^{-1}$ $cm.^{-1}$ as the molar absorptivity of ferric ions at 3050 Å and 25°C. With the above information, the cerous ion yields, from cobalt-60 gamma rays, for the ceric and

ceric-thallous dosimeters, were calculated and compared with values established by others, (see Results and Discussion section). If the comparison showed agreement to within 1%, the solutions were used in the cyclotron irradiations.

Analytical Methods for Proton-Irradiated Solutions. a. For Ferric Ions. One hundred milliliter samples of ferrous dosimeter solutions were irradiated with cyclotron-produced protons. Portions of these samples were analyzed for ferric ions as described above, using a Cary Model 11 MS spectrophotometer. From the increase in absorbance at 3050 Å affected by proton irradiation, the increase in ferric ion concentration was calculated using 2240 liters $mole^{-1}$ cm^{-1} as the molar absorptivity at 25°C, and a temperature coefficient of 0.7% per degree.[12]

b. For Ceric Ions. Ceric ion analysis has already been described for gamma irradiated solutions. The same procedure was used for proton irradiated solutions. The absorbance of ceric ion at 3200 Å is independent of temperature.

c. For Peroxysulfuric Acid. The radiation induced production of peroxysulfuric acid (H_2SO_5) in ceric solution has been discussed in detail by Boyle.[1] Peroxysulfuric acid was determined in this work in the following way. After the ceric sulfate dosimeter samples were analyzed for ceric ion remaining after irradiation, a few crystals of Baker and Adamson reagent grade ferrous ammonium sulfate were added. The sample was stirred or shaken to dissolve the crystals and the total oxidizing capacity of the sample was determined from

the amount of ferric ion produced in this operation. The analysis for ferric ion was performed as described above. Reaction of the ferrous ion with peroxysulfuric acid and ceric ion was quite rapid as indicated by the fact that the absorbance five minutes after addition of the ferrous salt was the same fifteen minutes later. Ferric ion is accurately measured spectrophotometrically in the presence of cerous ions because the molar absorptivity of the cerous ion is low.[16] From the difference between the molarity of ferric ions produced by the addition of the ferrous salt, and the molarity of ceric ions remaining after irradiation, (both values corrected from a blank sample) the normality of peroxysulfuric acid can be calculated, and from this the $G(H_2SO_5)$ can be computed (see eq. 41).

Cyclotron Irradiations. Irradiations were performed with the external, deflected beam of the Oak Ridge 86-inch cyclotron. Irradiation cells were placed at the end of an evacuated tube, approximately forty feet from the dees. Additional collimation was accomplished by a collimating system (Figures 3 and 4) arranged so that the diameter of the beam emerging from the thin aluminum window at the end of the evacuated tube was limited to one-eighth of an inch. Beam currents absorbed by the irradiation cell ranged from 0.5×10^{-9} to 4.0×10^{-9} amperes. The maximum available external beam current was approximately 10^{-7} amperes. The collimating system was designed in such a manner that if the beam passed through the collimator, it emerged through the center of the aluminum window at the end of the beam tube.

Solutions were irradiated in 250 ml. (tall form) beakers (Figures 2 and 4) provided with a one inch hole on the side. The proton beam entered the beaker through a one-half mil thick mylar window which was cemented over the opening with "Hysol" expoxy resin from Houghton Laboratories, Inc. Magnetic stirring was employed. Use of high stirring speeds and low beam current input insured that the measured yields were independent of stirring speed.[2,3] The adequacy of the stirring was established by increasing the stirring speed from zero until the ferric ion yield was found to be independent of further increase in the stirring speed. The rate of stirring was always maintained well above that rate at which $G(Fe^{+3})$ values were found to be independent of stirring speed. The radiation cells were reproducibly located by placing them at a measured distance from the window of the beam tube. In the early experiments, it was found that, if a beaker was inadvertently positioned so that the entire beam did not pass through the mylar window of the beaker, either the beaker or the expoxy resin became intensely colored, and these samples were discarded. Also, to insure that all of the beam passed into the irradiation cell through the thin mylar window on the cell, even after passing through the thickest aluminum absorber used in this work, the beam pattern was periodically checked with a zinc sulfide phosphor. One hundred milliliters of solution was pipetted into the beaker for each irradiation.

Measurement of Current Absorbed by the Solution. Two methods of current measurement were employed in the course of this investigation. The first method (Figure 2) utilized a platinum wire dipping into the solution as a charge collector. The wire was connected to a shielded coaxial cable leading to a current integrator. The proton beam was entirely stopped in the solution, and in the absence of electrical leaks, all of the charge passed to ground through the integrator. A test of this method of current measurement was made in the following manner.[4] During a normal irradiation at the maximum beam energy, a thin iron foil was placed in front of the cell window and exposed to an amount of beam which was measured with the current integrator through the platinum wire. A decay curve of the induced beta activity was obtained, and from the curve the amount of cobalt-55 (half-life equals 18 hours) produced by the irradiation was determined. Later, the same foil was irradiated with a similar amount of beam as measured by a rather elaborate Faraday cup arrangement. The beta activity was counted and decay curves used to determine the amounts of cobalt-55 which were produced. The same counter and lead shield were used and they were calibrated with the same standard source each time. The relative amounts of activity induced in the iron foil by a similar amount of beam in both cases was found to agree within 3% or less. Unfortunately, the current measuring technique using a platinum wire as a charge collector is susceptible to all of the difficulties mentioned by Allen,[5] such as scattering of secondary electrons

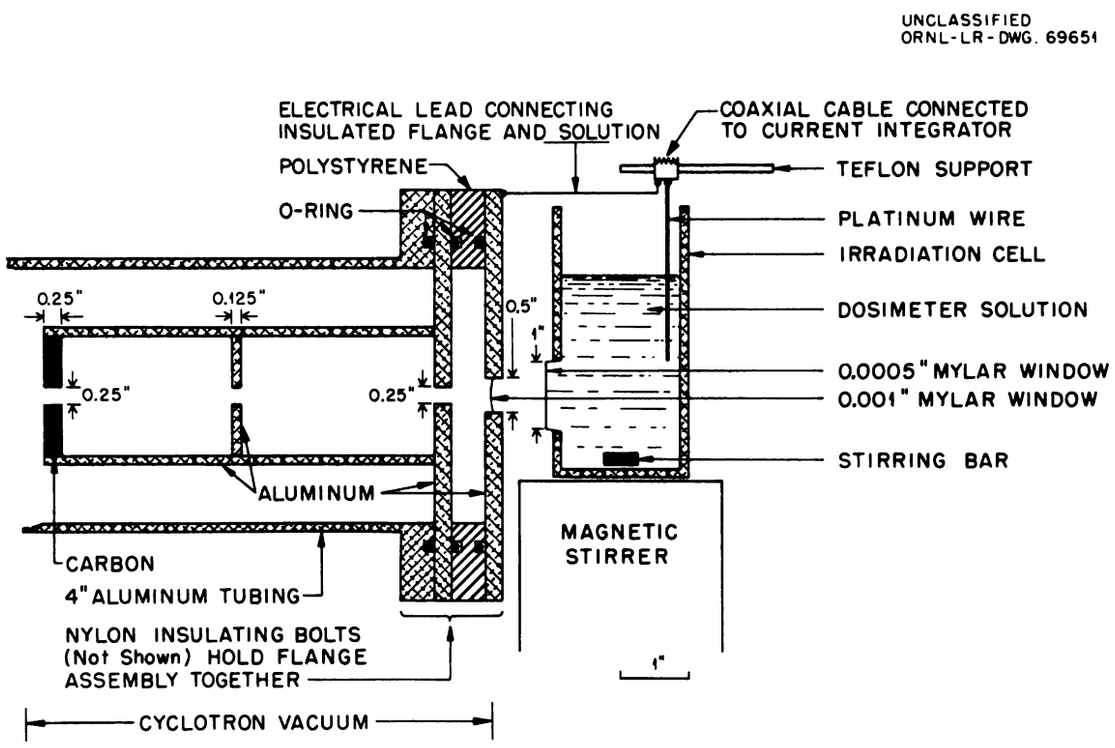

Figure 2. Experimental Arrangement Used for the Collection of Beam Currents from the 86-Inch Cyclotron.

produced by beam impinging on any surface, occurrence of electrical pathways from the solution to ground other than by the integrator (e.g., ionization of air by the beam), the charge transfer effect which is the ejection of secondary electrons in the direction of the primary beam from the thin insulating window of the cell into the solution, and other sources of error described in detail in various publications.[3,6,7,8,9,10] Although this technique worked well at or near the base beam energy of 23 Mev, the error in the measurement increased as the absorber thickness used to degrade the beam energy was increased. The sources of error were found to be intermittent, and not easily traceable. In the light of these difficulties this method of current measurement was finally abandoned.

The second method of current measurement (Figures 3, 4, 5) was virtually trouble-free due to the elimination of many of the sources of error inherent in the first method. This procedure involves two parts: the calibration and the measurement. Figure 3 represents the calibration procedure prior to the irradiation of a chemical solution. Beam passes through a nickel foil into a Faraday cup. Since the nickel foil is very thin (0.00005 inches or approximately 1.1 mg./cm^2) most of the proton beam passes through it into the Faraday cup where current produced by this beam is measured with a current integrator. A few protons per million are elastically scattered into the scintillation counter in proportion to the number

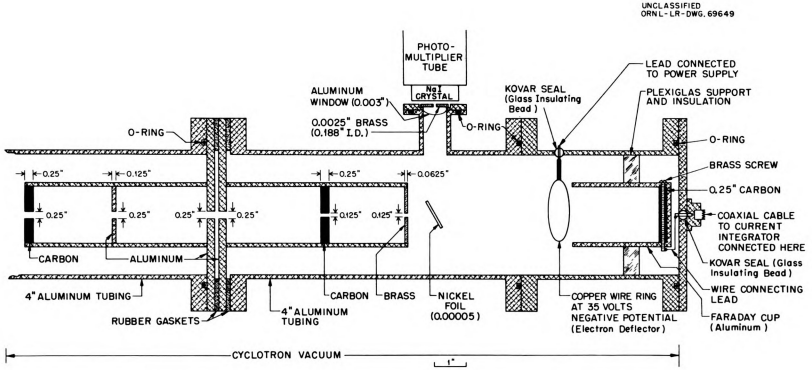

Figure 3. Experimental Arrangement Used for Measuring Beam Currents from the 86-Inch Cyclotron (Calibration Procedure).

of protons which pass through the nickel foil. Hence, in the absence of the Faraday cup (see Figure 4), one can calculate the current absorbed by a solution, or any other sample in which the beam is completely stopped, by knowing the ratio of the scintillation counts to the true counts as measured in the Faraday cup. To this end, a portion of the energy spectrum of protons scattered from the nickel foil, as recorded by a scintillation counter, (Figure 5), including the 2-plus peak (first excited state) and the elastic peak (ground state) was displayed on a 20-channel differential pulse height analyzer. The elastic peak was integrated by summation of all of the counts occurring in the channels above the appearance of the minimum between the first excited state peak and the elastic peak. Thus, by dividing the number of elastic peak counts by the number of microcoulombs, as measured with the Faraday cup, a ratio of peak counts per microcoulomb was established for the experiments to be run on that day. This calibration was performed at the beginning and end of each series of experiments, and the ratio was found to be constant at least over a twelve hour period. This method of current measurement is quite reliable if care is exercised in the geometrical design of the apparatus to insure that all of the proton beam which passed into the Faraday cup during the calibration, passes into the irradiation cell during solution irradiation. In addition, the method verified the contention expressed in the description of the first method of current

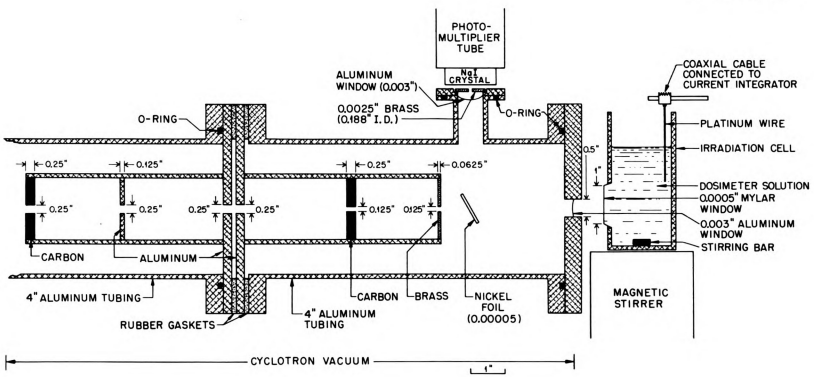

Figure 4. Experimental Arrangement Used for Irradiating Solutions with Protons from the 86-Inch Cyclotron (Method 2).

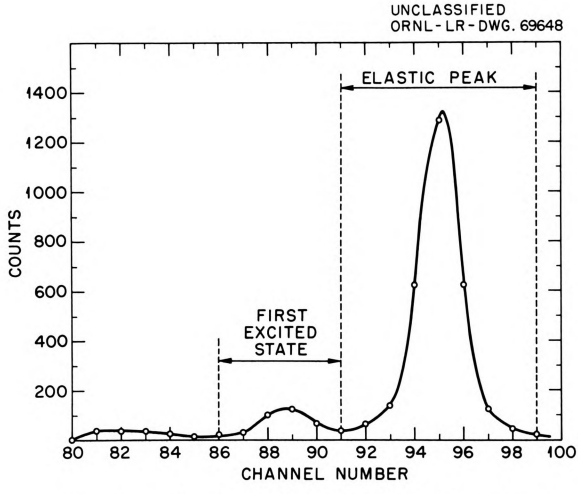

Figure 5. Portion of Nickel Scintillation Spectrum Used in Beam Current Measurement Procedure.

measurement attempted, that the platinum wire dipping into the solution did not provide a measure of the true proton beam current absorbed by the solution. A comparison of the current measured by both methods showed a 3% discrepancy at a beam energy of 23 Mev (no absorbers), and a gradual increase in the discrepancy up to 10 to 15% as the beam was degraded with absorbers down to 11 Mev.

Since the proton beam energy is degraded with absorbers, secondary electrons will be ejected from the absorbers and from the cell windows. The maximum energy of the electrons ejected from these absorber materials can be calculated by an application of the laws of conservation of total energy and conservation of momentum. The maximum energy imparted to an electron through a head-on collision with a 23 Mev proton is approximately 50 kev. The range of a 50 kev electron in aluminum is 0.0006 inches, and is approximately 0.001 inches in mylar (the cell window material). The average energy of the secondary electrons is considerably less than 50 kev. Even so, a 50 kev electron could not penetrate the cell window, and all secondary electrons entering the solution must be produced in the thin mylar window on the irradiation cell. As in earlier experiments with protons and deuteron beams,[2,3] it was assumed that the secondary electrons produced in the cell window are small in number and produce a negligible chemical change in the dosimeter solutions.

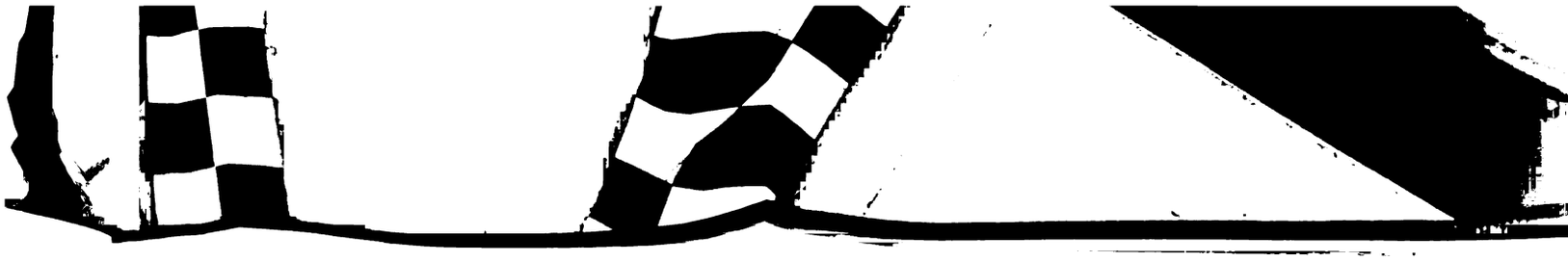

Experiments were conducted with an aluminum absorber 3 mg./cm.^{2} in excess of the proton beam range placed in front of the irradiation cell. Neither current absorption in, nor chemical change to the dosimeter solution was observed when this system was irradiated with 23 Mev protons. The significance of the experiment is that, although neutrons and γ-rays are emitted from the cyclotron, along with the protons they cause no measurable chemical change in the dosimeter solutions.

The current integrator used in this work was an instrument designed and constructed in the Instruments Division of the Oak Ridge National Laboratory. Briefly, it works on the following principle: the current to be measured is used to charge a condenser. At a pre-selected potential, an accurately known charge, opposite in sign to the charge on the condenser, is delivered to the condenser to discharge it back to its initial potential. These repetitive pulses, which are indicative of the charge, are counted with scalers so that the input charge is known to within 1% in the range 10^{-12} to 10^{-4} amperes.

The current integrator was calibrated at the beginning and end of each series of experiments with a calibration circuit which provided a current of 1 μamp. The calibration current was taken from a 100 volt source through large resistors. The accuracy of the instrument is no better than the stability of the 100 volt source, or the accuracy of the resistors considering their temperature coefficient. The calibration circuit was periodically tested

with an accurate voltmeter which was calibrated in the Instruments Division of the Oak Ridge National Laboratory. The reproducibility of these periodic tests substantiate the 1% estimation of the accuracy of the beam current measurements.

Measurement of Beam Energy. Beam energy measurement was a major consideration in this project. Although the Oak Ridge 86-inch cyclotron is designed to operate at a fixed frequency, and thus at constant energy, it was found that the beam energy is subject to periodic variations depending on the operating conditions. Until this situation was realized, the accumulation of reliable data was seriously hampered. For this reason, the beam energy was measured periodically during each series of experiments.

The procedure used for beam energy measurement is similar to that described in various publications.[2,8,11] The usual procedure for beam energy measurements involves the determination of the range of the beam in aluminum absorbers. This involves passing the beam into increasing amounts of absorber until the beam is just stopped in the absorber. This method was considered too tedious for routine measurement of beam energies and although the range-energy relationship was maintained as the primary standard, the range in aluminum was determined by a faster, indirect method. The range of the beam was measured by passing it through enough aluminum absorber to degrade the beam energy approximately 74-76%. The residual energy was estimated from the amount of oxidation produced in a ferrous sulfate dosimeter

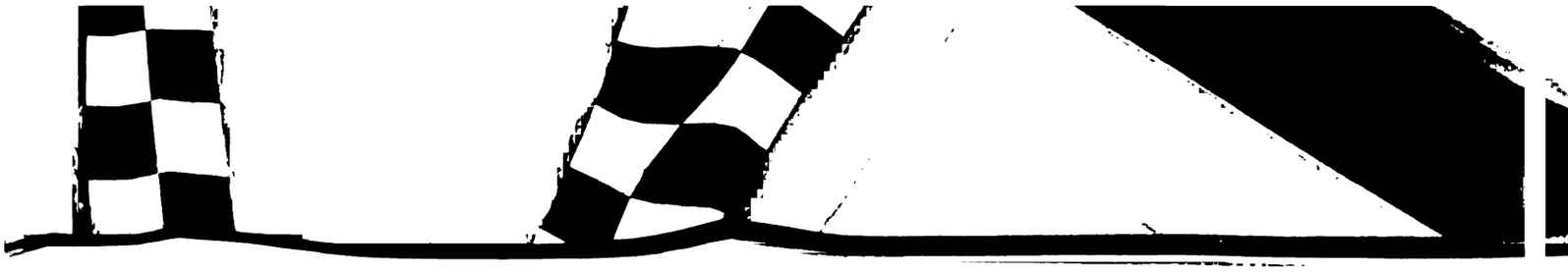

(see Figure 6). The degradation of the beam energy by 74-76% was selected as a compromise in minimizing the effects of beam scattering and misalignment of the absorber while insuring that the energy was in the range where ferrous oxidation yields are well known. The fraction of the range expended in the solution is small so that a relatively large error in the assumed value of the ferrous oxidation yield for the residual energy produces a small error in the total range. For example, in an energy measurement in which the base beam energy is determined to be 23.2 Mev, and the residual energy as 6 Mev, a 5% error in the determination of residual energy corresponds to 0.3 Mev in 6 Mev or 0.3 Mev in 23.2 Mev indicating that the total error in the base beam energy measurement is approximately 1%. A more realistic figure for the error in the determination of the residual energy is 1-2%, (estimation of the accuracy of known ferrous oxidation yields) which results in a base beam energy measurement error of 0.6%. For a similar method of energy measurement, Allen[8] estimated the accuracy to $\pm$ 0.3%.

The method for computation of beam energy was derived as follows. The base proton beam energy was assumed to be greater than 22 Mev and less than 24 Mev.[66] A base beam energy in this region was assumed, and the total range of this beam in aluminum was found from range-energy curves.[15] Since the beam passed through a known thickness of aluminum absorber, a residual range and hence an estimated residual energy could be deduced from range-energy curves. A $G(Fe^{+3})$ value was calculated using the

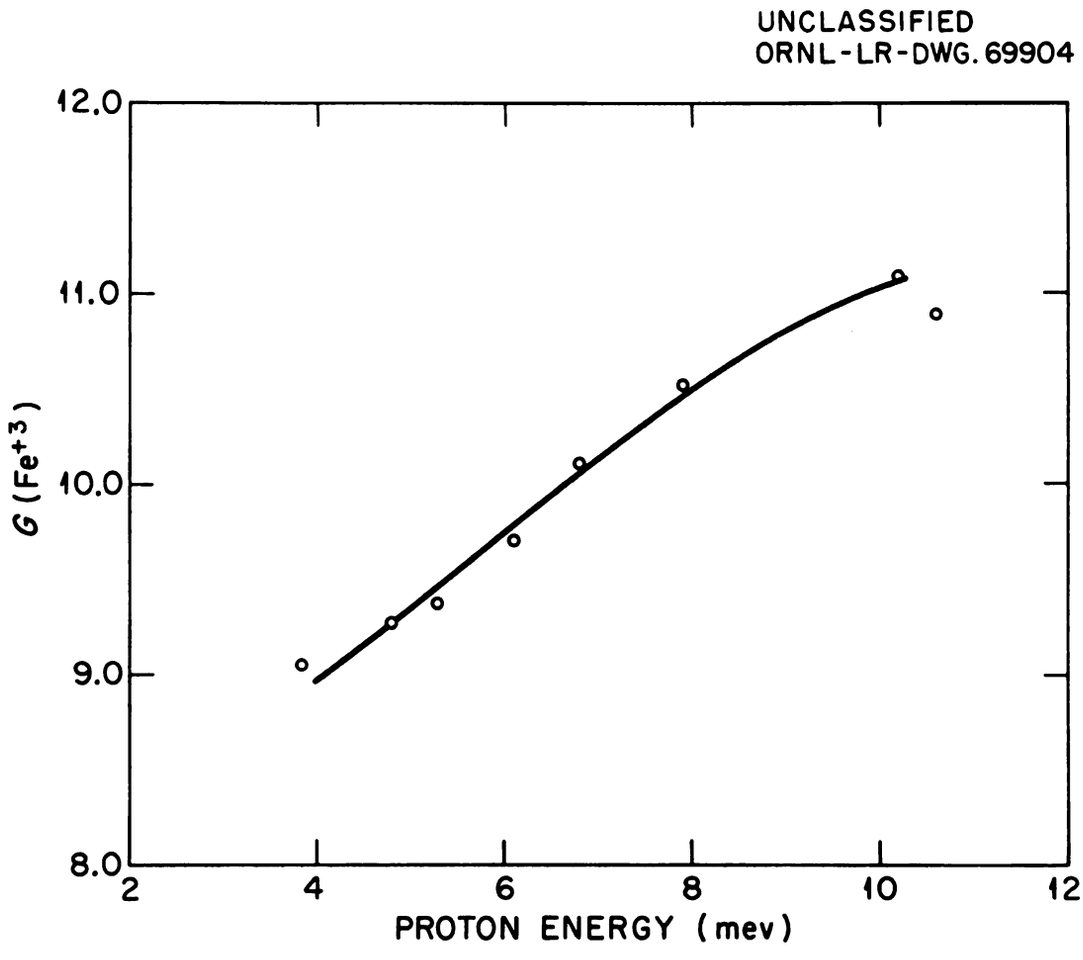

Figure 6. Known Ferric Ion Yields versus Proton Energy (See Reference 3).

estimated residual energy, and the measured values of the number of ferric ions produced and the μcoulombs absorbed in the solution according to equation (41), where μcoul proton^{-1} equals 1.602 x 10^{-13}.

$$(41)\quad G = \frac{\text{No. product ions produced x } \mu\text{coul proton}^{-1}}{\mu\text{coul absorbed x Mev proton}^{-1} \text{ x 100 ev Mev}^{-1}}$$

If the calculated G(Fe^{+3}) and the estimated value for the residual energy did not fall on Figure 6, the plot of known ferric ion yields versus energy, another base beam energy was assumed, and the calculation was repeated until a unique solution for G(Fe^{+3}) and the estimated residual energy, corresponding to a point on Figure 6, was found. The assumed base proton beam energy which led to this unique solution for G(Fe^{+3}) and the estimated residual energy was taken as the true value of the base proton beam energy.

Proton beam energies determined in the above manner were compared with independent measurements made by the Nuclear Physics Group at the Oak Ridge National Laboratory[65] (see Table I). Briefly, the method involved the degradation of the beam energy with aluminum absorbers until the response of a silicon-surface barrier counter was the same as that produced by α-particles of known energy.

It should be noted that Figure 6 was prepared using the data of Hart and co-workers,[3,10] and not that of Schuler and Allen.[2] The main reason for this choice is the excellent agreement between beam energy values determined in this study, and those determined by an independent measurement,[65] which was obtained when the data

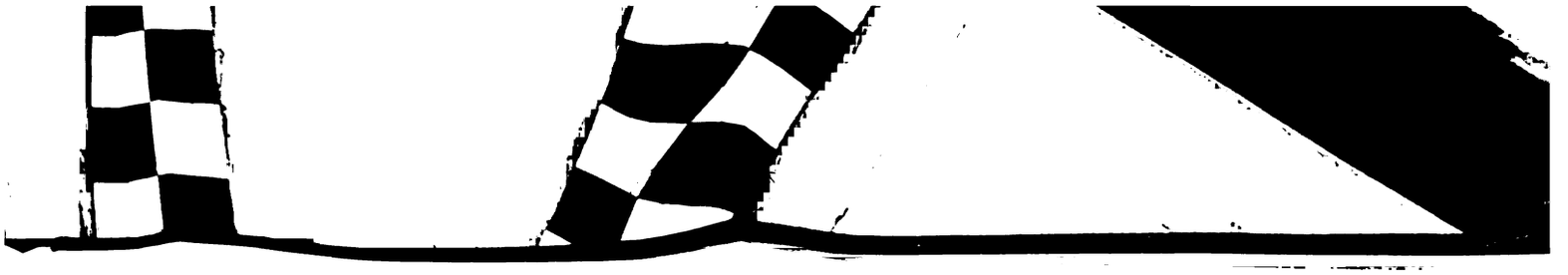

of Hart and co-workers was used in the preparation of Figure 6. Even so, if the data of Schuler and Allen were used in preparing Figure 6, values of the base beam energy shown in Table I would be lowered only 1%. This corresponds to a 1% increase in the G values at 23 Mev and a 3% increase at 11 Mev. Thus, even if the data of Schuler and Allen were used in preparing Figure 6, the data of the present investigation would fit smoothly as an extension of the data of Hart and Anderson (see Figure 7).

V. RESULTS AND DISCUSSION

Beam Energy Measurements. Experimentally determined values for the proton beam energy of the Oak Ridge 86-inch cyclotron are tabulated and compared with independent measurements in Table I. The theory, technique and reliability of these measurements has been discussed in detail in the Experimental section.

Cerous Ion Yields Produced by Cobalt-60 Gamma Irradiation. As stated in the Experimental section, the ferrous dosimeter is an easily prepared and fairly reliable dosimeter even in the presence of small amounts of impurities. However, the ceric and ceric-thallous dosimeters are quite sensitive to impurities. Therefore, in addition to the precautions exercised in the preparation of these solutions, they were irradiated in a Co-60 γ-source in order to check their rate of decomposition under irradiation against well-established rate values. The most reliable value for the cerous ion yield appears to be that recorded in an exhaustive study by Boyle.[1] He finds $G(Ce^{+3})$ for aerated ceric solutions to be 2.47. The theoretical yield for cerous ion from the ceric-thallous dosimeter (thallous ion concentration equal to 10^{-5} to 10^{-2} M) is 8.18. Although Sworski[13] obtained a value of 7.92, others[14] have obtained 8.18 ± 0.02. Yields obtained for solutions used in this work are tabulated in Table II. The agreement of these experimentally determined cerous ion yields, with values reported by others,[1,14] was selected as the criterion for the reliability of the solutions in further radiolysis studies.

Table I. Experimentally Determined 86-Inch Cyclotron Proton Beam Energies

Date (1962)	Air Traversed By Beam (cm)	$G(Fe^{+3})$[a]	Residual[b] Energy (Mev)	Residual Range mg/cm^2Al	Total Range mg/cm^2Al	Charge Input to Soln. (μcoul)	Fe^{+3} Produced x 10^{-18}	Base[c] Beam Energy (Mev)
4-16	0.5	9.97	6.32	76	740	3.445	13.56	23.25
4-16	0.5	9.97	6.74	84	748	3.236	13.57	23.40
4-16	0.5	9.97	6.68	83	747	3.059	12.71	23.37
4-16	0.5	9.97	6.75	84	748	1.233	5.177	23.40
4-25	0.5	9.60	5.54	61	725	2.031	6.752	22.95
5-3	3.8	9.80	6.23	74.5	738.5	2.000	7.619	23.3
5-3	3.8	9.70	5.89	68	732	2.098	7.481	23.2
5-9	3.8	9.53	5.39	59	723	1.952	6.258	23.0
5-9	3.8	9.50	5.33	58	722	1.927	6.095	23.0
5-9	3.8	9.55	5.47	60	724	1.887	6.149	23.0
5-9	3.8	9.52	5.37	59	723	2.886	9.203	23.0
5-9	3.8	9.47	5.23	57	721	2.953	9.119	23.0
4-23	-	-	-	-	-	-	-	23.2*
5-8	-	-	-	-	-	-	-	22.9*

*Independent measurements using another method by the Nuclear Physics Group, Electronuclear Research Division, Oak Ridge National Laboratory.[65]

[a]Best estimate of $G(Fe^{+3})$ obtained as described in Results and Discussion section.

[b]After passing through 664 mg/cm^2 of aluminum.

[c]Corrected for energy loss in air.

Table II. Cerous Ion Yields Produced by Cobalt-60 Gamma Rays

Run	Dose Rate (ev ml^{-1} min^{-1} x 10^{-16})	Dosimeter	G(ions/100 ev)*
1	6.60	Ceric	2.48 ± .02
2	6.02	Ceric	2.49 ± .02
3	6.00	Ceric-Thallous	8.20 ± .02
4	5.99	Ceric-Thallous	8.19 ± .02

*Each value is an average of six determinations.

Ferric Ion Yields for Cyclotron-Produced Protons. Experimentally determined ferric ion yields for 11-23 Mev protons are tabulated in Tables III, VII, VIII and IX and are shown graphically in Figures 7 and 8. The yields are given as $G(Fe^{+3})$, which is defined as the average ferric ion yield per 100 ev of energy absorbed. Figure 7 provides a comparison of yields obtained in the work with those of other workers. In this figure, $G(Fe^{+3})$ is plotted against reciprocal LET_i, $-(dx/dE)_i$. There is good agreement among replicate values, which extrapolate smoothly to the data of Anderson and Hart[3] but not to the data of Schuler and Allen.[2] At higher proton and deuteron energies, (LET range ~ 0.45 to 0.9 ev/Å) a 6% discrepancy between the data of Anderson and Hart and that of Schuler and Allen has been noted in various publications by these authors,[2,3,10] but no satisfactory explanation for the discrepancy has been proposed. The Schuler and Allen,[2] and Barr and Schuler[17] values, plotted on Figure 7, are ones read off directly from the graphs reproduced in their publications, and are not individual experimental values.

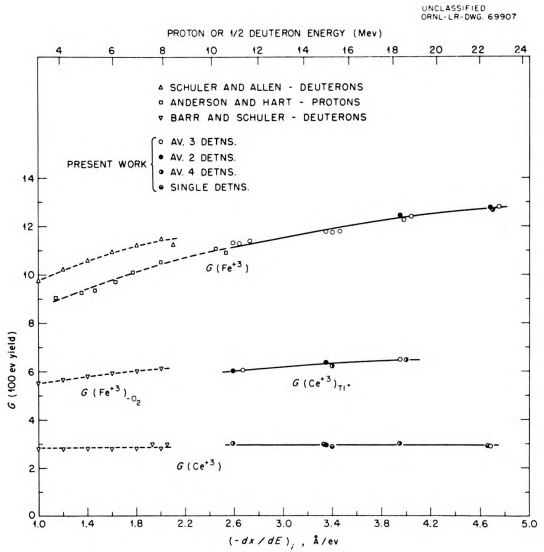

Figure 7. Experimental Yields as Related to Reciprocal LET_i in the Proton and Deuteron Radiolysis of Ferrous and Ceric Solutions.

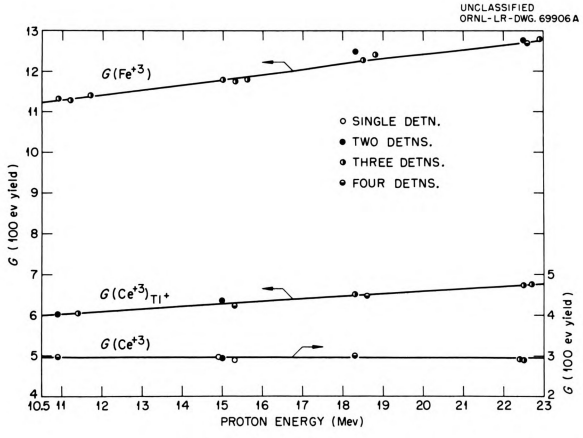

Figure 8. Experimental Yields in the Proton Radiolysis of Ferrous and Ceric Solutions.

Table III. $G(Fe^{+3})$ Values from the Radiolysis of Aerated, Acidified Ferrous Sulfate Solutions

Run	Molecules Fe^{+3} Produced x 10^{-18}	μcoul Absorbed	Proton Energy (Mev)	Electron Volts Absorbed x 10^{-19}	$G(Fe^{+3})$
1	20.06	1.134	22.62	16.00	12.54
2	19.54	1.085	22.62	15.31	12.76
3	20.78	1.145	22.62	16.17	12.85
4	20.22	1.136	22.62	16.03	12.61
5	15.50	1.119	18.52	12.92	12.00
6	16.30	1.141	18.52	13.19	12.36
7	16.33	1.135	18.52	13.12	12.45
8	12.27	1.118	15.25	10.65	11.52
9	13.10	1.146	15.25	10.91	12.01
10	12.74	1.129	15.25	10.75	11.85
11	8.914	1.127	11.21	7.886	11.30
12	9.185	1.177	11.21	8.229	11.16
13	8.944	1.123	11.21	7.859	11.38
14	21.15	1.158	22.92	16.57	12.76
15	21.03	1.151	22.92	16.47	12.77
16	21.51	1.172	22.92	16.77	12.83
17	16.80	1.149	18.81	13.49	12.45
18	16.76	1.161	18.81	13.63	12.30
19	19.06	1.305	18.81	15.32	12.44
20	13.96	1.194	15.62	11.64	11.99
21	14.02	1.210	15.62	11.80	11.88
22	13.58	1.212	15.62	11.82	11.49
23	10.01	1.206	11.68	8.793	11.38
24	10.08	1.216	11.68	8.866	11.37
25	9.974	1.195	11.68	8.713	11.45
26	20.26	1.131	22.48	15.87	12.77
27	20.32	1.136	22.48	15.94	12.75
28	15.17	1.056	18.33	12.08	12.56
29	14.60	1.031	18.33	11.80	12.37
30	15.59	1.417	14.98	13.25	11.77
31	15.76	1.440	14.98	13.46	11.70
32	15.65	1.408	14.98	13.17	11.88
33	11.20	1.440	10.94	9.834	11.39
34	11.09	1.436	10.94	9.806	11.31
35	10.85	1.412	10.94	9.642	11.25

As expected, Figure 7 indicates decreasing ferric ion yields for increasing LET due to increasing radical recombination.

Proton Induced Cerous Ion Yields in the Presence of Thallous Ions. $G(Ce^{+3})_{Tl^+}$ yields for 11-23 Mev protons are tabulated in Tables IV, VII, VIII and IX, and are represented graphically in Figures 7 and 8. The $G(Ce^{+3})_{Tl^+}$ values obtained in this study may be compared directly with the $G(Fe^{+3})_{-O_2}$ values obtained by Barr and Schuler[17] since, as pointed out in the Theory section, they are numerically equivalent (c.f., equations (25) and (35)).

The $G(Ce^{+3})_{Tl^+}$ data from the present work does not extrapolate into that of Barr and Schuler,[17] for $G(Fe^{+3})_{-O_2}$, however, the disagreement in this case appears to be the same order of magnitude noted in the comparison of the two sets of data for $G(Fe^{+3})$, (approximately 6%).

$G(Ce^{+3})_{Tl^+}$ decreases with increasing LET for the same reason cited in the discussion of $G(Fe^{+3})$ yields.

Cerous Ion Yields for Cyclotron-Produced Protons. $G(Ce^{+3})$ yields for 11-23 Mev protons are given in Tables V, VII, VIII and IX and are shown graphically in Figures 7 and 8. Because of the opposing radical reactions in the radiolysis of ceric solutions, (reduction by H and oxidation by OH) the yields for this solute are small, and result primarily from the reduction of ceric ions by H_2O_2. Since $G_{H_2O_2}$ does not change rapidly with LET, $G(Ce^{+3})$ would not be expected to change rapidly. As indicated on Figures 7 and 8, $G(Ce^{+3})$ appears to be virtually constant at 2.95 in the LET range from 0.2 to 0.4 ev/Å.

Table IV. $G(Ce^{+3})_{Tl^+}$ Values from the Radiolysis of Aerated, Acidified Ceric + Thallous Sulfate Solutions

Run	Molecules Ce^{+4} x 10^{-18} Depleted	μcoul Absorbed	Proton Energy (Mev)	Electron Volts Absorbed x 10^{-19}	$G(Ce^{+3})_{Tl^+}$
52	13.64	1.420	22.73	20.15	6.77
53	16.06	1.686	22.73	23.92	6.71
54	13.88	1.443	22.73	20.47	6.78
55	11.09	1.469	18.58	17.04	6.50
56	10.86	1.449	18.58	16.81	6.46
57	10.91	1.464	18.58	16.98	6.43
58	10.96	1.457	18.58	16.90	6.48
59	10.40	1.745	15.34	16.71	6.22
60	8.601	1.452	15.34	13.90	6.19
61	8.998	1.511	15.34	14.47	6.22
62	8.926	1.498	15.34	14.34	6.22
63	6.613	1.545	11.36	10.96	6.03
64	6.649	1.556	11.36	11.03	6.03
65	7.101	1.649	11.36	11.69	6.07
66	13.32	1.402	22.48	19.67	6.77
67	13.07	1.397	22.48	19.60	6.67
68	15.40	1.632	22.48	22.90	6.72
69	10.37	1.406	18.33	16.08	6.45
70	10.40	1.409	18.33	16.12	6.45
71	9.998	1.332	18.33	15.24	6.56
72	8.354	1.414	14.98	13.22	6.32
73	8.390	1.411	14.98	13.19	6.36
74	5.703	1.389	10.94	9.485	6.01
75	6.228	1.518	10.94	10.37	6.01

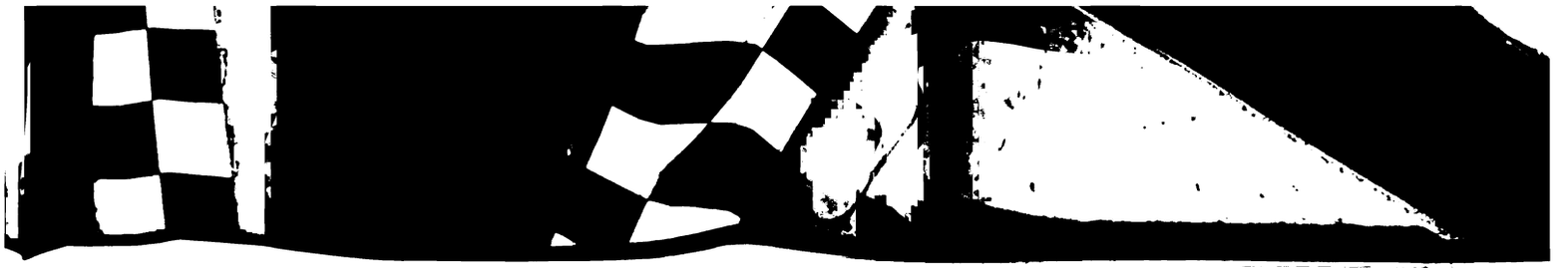

Table V. $G(Ce^{+3})$ Values from the Radiolysis of Aerated, Acidified Ceric Sulfate Solutions

Run	Molecules Ce^{+4} x 10^{-18} Depleted	μcoul Absorbed	Proton Energy (Mev)	Electron Volts Absorbed x 10^{-19}	$G(Ce^{+3})$
36	7.776	1.885	22.46	26.43	2.94
37	6.800	1.667	22.40	23.31	2.92
38	6.860	1.978	18.26	22.55	3.04
39	5.799	1.682	18.26	19.17	3.02
40	4.392	1.595	14.91	14.84	2.96
41	3.866	1.917	10.86	13.00	2.97
42	1.901	0.9293	10.86	6.300	3.02
43	7.366	1.809	22.48	25.38	2.90
44	7.197	1.811	22.48	25.41	2.83
45	6.119	1.783	18.33	20.40	3.00
46	6.119	1.823	18.33	20.86	2.93
47	5.305	1.916	14.98	17.92	2.96
48	5.080	1.880	14.98	17.58	2.89
49	3.813	1.869	10.94	12.76	2.99
50	3.737	1.875	10.94	12.80	2.92
51	4.027	1.460	15.34	13.98	2.88

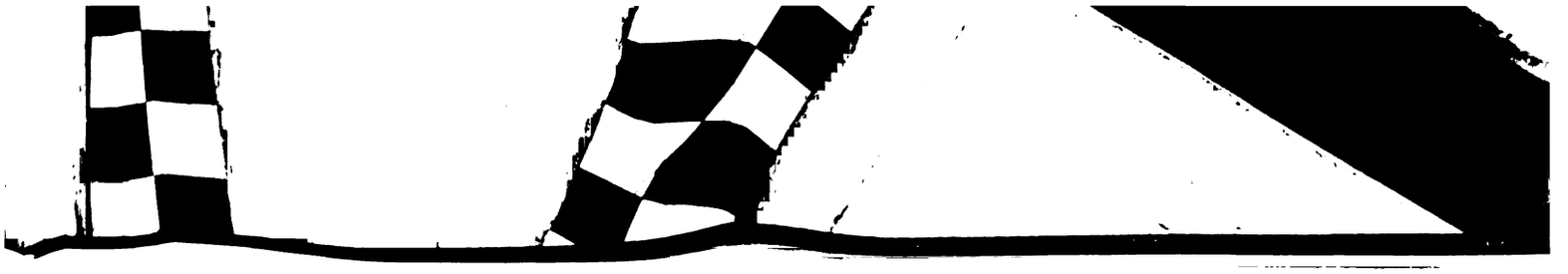

The $G(Ce^{+3})$ values reported by Barr and Schuler[17] decrease from 2.80 to 2.78 as LET_i is decreased from 1.0 to 0.5 ev/Å. Other data (see reference 5) have been reported, indicating a maximum in the cerous yield of 3.2 at 0.2 ev/Å. Clearly, the over-all trend of $G(Ce^{+3})$ variation as a function of LET has not been well established. Additional work in the entire LET range is needed, and especially in the region from 0.02 to 1.0 ev/Å where a discrepancy in $G(Ce^{+3})$ yields does exist. It might be pointed out, that the $G(Ce^{+3})$ value obtained by Barr and Schuler at a LET of 0.5 ev/Å, differs from the 2.95 value of the present work by 6%.

Peroxysulfuric Acid Yields. As shown by Boyle,[1] peroxysulfuric acid is formed and accumulates during radiolysis of ceric sulfate solutions. Values of $G(H_2SO_5)$, obtained in this study, are tabulated in Table VI. Because these yields are small, they are difficult to obtain with greater precision than that exhibited in Table VI. Boyle,[1] reported a $G(H_2SO_5)$ value of $0.14 \pm .02$ for cobalt-60 gamma radiolysis (LET_i = 0.02 ev/Å) under more rigidly controlled experimental conditions. The average $G(H_2SO_5)$ for 11-23 Mev protons, from Table VI is 0.16. $G(H_2SO_5)$ would be expected to exhibit a greater increase with increasing LET, thus 0.16 is assumed to be a low estimate of $G(H_2SO_5)$ in the 0.2 to 0.4 ev/Å LET region. The inclusion of $G(H_2SO_5)$ in the calculation of molecular and free radical yields results in the respective yields tabulated in Table IX. A comparison of

Table VI. $G(H_2SO_5)$ Values from the Radiolysis of Aerated, Acidified Ceric Sulfate Solutions

Run	$\underline{M}$ Ce^{+3} after irr. x 10^4	$\underline{M}$ Fe^{+3} after Fe^{+2} addn. x 10^4	$\underline{N}$ H_2SO_5 (equiv/) x 10^6	H_2SO_5 equiv. molecules produced x 10^{-16}	Electron Volts Absorbed x 10^{19}	Proton Energy (Mev)	$G(H_2SO_5)$*
36	3.643	3.745	10.2	61.43	25.81	22.46	0.24
37	3.806	3.862	5.60	33.73	23.31	22.40	0.145
38	3.795	3.853	5.80	34.93	21.99	18.26	0.16
39	3.971	4.001	3.00	18.07	19.28	18.26	0.094
40	4.205	4.256	5.10	30.72	14.84	14.91	0.21
41	4.292	4.315	2.30	13.85	13.00	10.86	0.11
42	4.619	4.633	1.40	8.432	6.198	10.86	0.14

*Expressed in equivalent molecules of H_2SO_5 per 100 electron volts absorbed.

Tables VIII and IX indicates the magnitude of change in yields caused by this refinement.

Molecular and Free Radical Yields. A complete analysis of the data into primary molecular and free radical yields is given in Tables VIII and IX. Values listed for ferric and cerous ion yields were taken from Figure 8, which is a plot of radiolysis yields obtained in this study versus proton energy. This operation was necessary in order to obtain cerous and ferric ion yields at specific proton energies, because, due to variations in the base beam energy of the cyclotron, the various yields could not be measured at exactly the same proton energy. Figure 8 is drawn with sufficient care, so that $G(Fe^{+3})$, $G(Ce^{+3})_{Tl^+}$, and $G(Ce^{+3})$ may be obtained directly at any proton energy between 10.5 and 23 Mev.

Table VIII represents an analysis of the data into molecular and free radical yields neglecting the formation of H_2SO_5, while Table IX represents the results when H_2SO_5 formation is considered.

G_H, G_{OH}, $G_{H_2O_2}$, G_{H_2}, and G_{-H_2O} in Table VIII were calculated from $G(Fe^{+3})$, $G(Ce^{+3})_{Tl^+}$, and $G(Ce^{+3})$ by assuming the relationships between the experimental yields and the primary intermediate yields expressed in equations (7), (23), (32), and (35).

(7) $G_{-H_2O} = G_H + 2G_{H_2} = G_{OH} + 2G_{H_2O_2}$

(23) $G(Fe^{+3}) = 2G_{H_2O_2} + 3G_H + G_{OH}$

(32) $G(Ce^{+3}) = 2G_{H_2O_2} + G_H - G_{OH}$

(35) $G(Ce^{+3})_{Tl^+} = 2G_{H_2O_2} + G_H + G_{OH}$

Table VII. Summary of $G(Fe^{+3})$, $G(Ce^{+3})$ and $G(Ce^{+3})_{Tl^+}$ Values Obtained in This Investigation

Proton Energy (Mev)	$G(Fe^{+3})$	Proton Energy (Mev)	$G(Ce^{+3})$	Proton Energy (Mev)	$G(Ce^{+3})_{Tl^+}$
22.9	12.76	22.5	2.90	22.7	6.77
22.9	12.77	22.5	2.83	22.7	6.71
22.9	12.83	22.5	2.94	22.7	6.78
22.6	12.54	22.4	2.92	22.5	6.77
22.6	12.76	18.3	3.00	22.5	6.67
22.6	12.85	18.3	2.93	22.5	6.72
22.6	12.61	18.3	3.04	18.6	6.50
22.5	12.77	18.3	3.02	18.6	6.46
22.5	12.75	15.3	2.88	18.6	6.43
18.8	12.45	15.0	2.96	18.6	6.48
18.8	12.30	15.0	2.89	18.3	6.45
18.8	12.44	14.9	2.96	18.3	6.45
18.5	12.00	10.9	2.99	18.3	6.56
18.5	12.36	10.9	2.92	15.3	6.22
18.5	12.45	10.9	2.97	15.3	6.19
18.3	12.56	10.9	3.02	15.3	6.22
18.3	12.37			15.3	6.22
15.6	11.99			15.0	6.32
15.6	11.88			15.0	6.36
15.6	11.49			11.4	6.03
15.3	11.52			11.4	6.03
15.3	12.01			11.4	6.07
15.3	11.69			10.9	6.01
15.0	11.77			10.9	6.01
15.0	11.70				
15.0	11.88				
11.7	11.38				
11.7	11.37				
11.7	11.45				
11.2	11.30				
11.2	11.15				
11.2	11.38				
10.9	11.39				
10.9	11.31				
10.9	11.25				

Table VIII. Molecular and Free Radical Yields from the Radiolysis of Ferrous and Ceric Solutions. Peroxysulfuric Acid Yield Neglected

E_P (Mev)	$G(Fe^{+3})$	$G(Ce^{+3})_{Tl^+}$	$G(Ce^{+3})$	G_H	G_{OH}	$G_{H_2O_2}$	G_{H_2}	G_{-H_2O} [a]	G_{HOH} [b]	$G_{-H_2O(T)}$ [c]	X [d]
22.0	12.64	6.71	2.95	2.97	1.88	0.93	0.39	3.74	1.32	5.06	0.48
22.0	12.41	6.58	2.95	2.92	1.82	0.92	0.37	3.66	1.29	4.95	0.48
18.0	12.18	6.46	2.95	2.86	1.76	0.92	0.37	3.60	1.29	4.89	0.47
16.0	11.91	6.33	2.95	2.79	1.69	0.93	0.38	3.54	1.31	4.85	0.46
14.0	11.65	6.21	2.95	2.72	1.63	0.93	0.39	3.49	1.32	4.81	0.45
12.0	11.42	6.07	2.95	2.68	1.56	0.92	0.36	3.39	1.28	4.67	0.45
10.5	11.22	5.98	2.95	2.62	1.52	0.92	0.37	3.36	1.29	4.65	0.44_5

[a] Calculated from equation (7), $2G_{H_2} + G_H$.

[b] Yield of water from recombination of H and OH.

[c] Sum of columns 9 and 10.

[d] X equals fraction of radicals combining with solute, $G_H + G_{OH}/2G_{-H_2O(T)}$.

Table IX. Molecular and Free Radical Yields from the Radiolysis of Ferrous and Ceric Solutions. Peroxysulfuric Acid Yield Considered

E_P (Mev)	$G(Fe^{+3})$	$G(Ce^{+3})_{Tl^+}$	$G(Ce^{+3})$	$G(H_2SO_5)$[a]	G_H	G_{OH}	$G_{H_2O_2}$	G_{H_2}	G_{-H_2O}[b]	G_{HOH}[c]	$G_{-H_2O(T)}$	X[e]
22.0	12.64	6.71	2.95	0.16	2.97	1.72	0.85	0.38	3.73	1.23	4.96	0.47
20.0	12.41	6.58	2.95	0.16	2.92	1.66	0.84	0.37	3.65	1.21	4.86	0.47
18.0	12.18	6.46	2.95	0.16	2.86	1.60	0.84	0.37	3.60	1.21	4.81	0.46
16.0	11.91	6.33	2.95	0.16	2.79	1.53	0.85	0.38	3.54	1.23	4.77	0.45
14.0	11.65	6.21	2.95	0.16	2.72	1.47	0.85	0.39	3.49	1.24	4.73	0.44
12.0	11.42	6.07	2.95	0.16	2.68	1.40	0.83	0.35	3.38	1.18	4.56	0.45
10.5	11.22	5.98	2.95	0.16	2.62	1.36	0.84	0.37	3.36	1.21	4.57	0.43[d]

[a] Average value taken from Table V.

[b] Calculated from equation (7), $G_H + 2G_{H_2}$

[c] Yield of water formed from recombination of H and OH.

[d] Sum of columns 9 and 10.

[e] X equals the fraction of radicals combining with solute or $G_H + G_{OH}/2G_{-H_2O(T)}$.

The primary intermediate yields in Table IX were calculated by assuming the relationships expressed in equations (32), (42), (43),

(42) $G_{-H_2O} = G_H + 2G_{H_2} = G_{OH} + 2G_{H_2O_2} + 2G_{H_2SO_5}$

(43) $G(Fe^{+3}) = 2G_{H_2O_2} + 3G_H + G_{OH} + 2G_{H_2SO_5}$

and (44). $G(H_2SO_5)$ is included in the latter three equations because,

(44) $G(Ce^{+3})_{Tl^+} = 2G_{H_2O_2} + G_H + G_{OH} + 2G_{H_2SO_5}$

in 0.4 M H_2SO_4, H_2SO_5 reacts as an oxidizing agent. In ceric sulfate solutions, however H_2SO_5 accumulates, and does not react; therefore, it need not be considered as a contribution to $G(Ce^{+3})$ yields. In the absence of direct experimental evidence, it was assumed that H_2SO_5 oxidizes two thallous ions to Tl^{+2} ions which react with two ceric ions, producing two cerous ions. This appears to be a good assumption in view of the fact that $G(Fe^{+3})_{-O_2}$ is equivalent to $G(Ce^{+3})_{Tl^+}$.

The free radical yields, G_H and G_{OH}, decrease with increasing LET, as expected (see Tables VIII and IX). The G_H values show almost exact agreement with estimations made by Allen, (see reference 5, page 58) from available data. Caution should be exercised in comparing the present work with that of other investigators. In publications where H_2SO_5 formation is not considered, Table VIII should be used for the comparison.

The G_{OH} values (Table VIII) of the present study are lower than those estimated in Allen's graph. The disagreement in this case is not surprising however, since G_{OH} values are usually

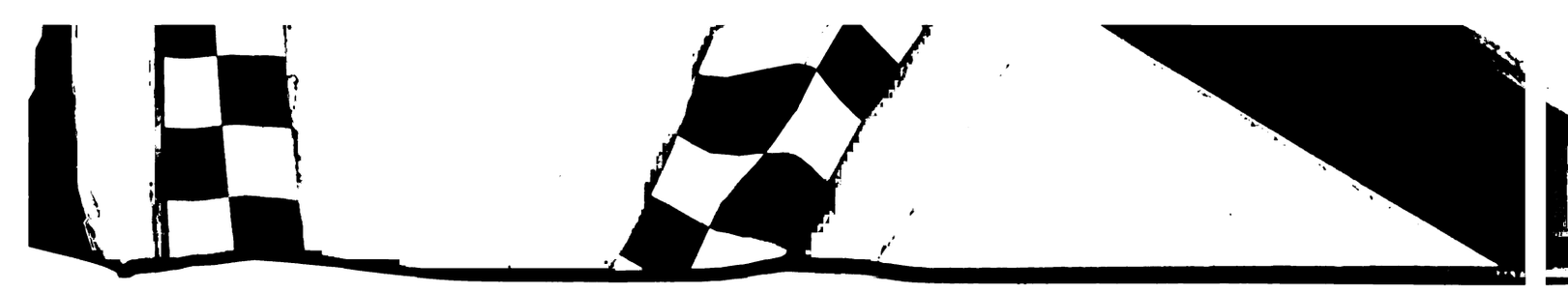

estimated from $G(Ce^{+3})$ values, and as mentioned previously, there is considerable disagreement in the literature over the correct $G(Ce^{+3})$ value at various values for LET.

The G_H yields of this study were calculated from the difference between $G(Fe^{+3})$ and $G(Ce^{+3})_{Tl}+$ yields. The excellent agreement of the present G_H yields with those calculated by others verifies the credibility of the experimental $G(Fe^{+3})$ and $G(Ce^{+3})_{Tl}+$ yields of this study. The G_{OH} yields were calculated from the difference between $G(Fe^{+3})$ and $G(Ce^{+3})$ and from the calculated value of G_H. The disagreement of the G_{OH} values with those of others indicates an error in $G(Ce^{+3})$ yields in the present work, or in the published values. The discrepancy between $G(Ce^{+3})$ values of the present work and those reported by others is approximately 6% at LET equal to 0.4 ev/Å, and about 8% at 0.2 ev/Å. ($G(Ce^{+3})$ values in Table VIII are too high according to Barr and Schuler[17] and too low according to Hardwick).[53] Additional work is required before the $G(Ce^{+3})$ and G_{OH} values can be unequivocably established.

The molecular yields, G_{H_2} and $G_{H_2O_2}$ remain essentially constant as LET is varied from 0.2 ev/Å to 0.4 ev/Å but should increase slightly with increasing LET. Neither of these yields can be calculated according to the method of this report without inheriting the apparent errors in $G(Ce^{+3})$ and/or G_{OH}. The $G_{H_2O_2}$ values (Table VIII) are approximately the correct order of magnitude, (Allen estimates $G_{H_2O_2} = 0.98$ at 0.2 ev/Å). The greatest deviation from

expected yields lies in the G_{H_2} values which are lower than expected. The reason for the large error in this value is two-fold: (1) Since this value is numerically small, and is obtained by difference, small errors in the numbers to be subtracted result in a large error in the resultant difference. (2) G_{H_2} was obtained from the equation of material balance; therefore, all errors inherent in the raw data and in other calculated values, accumulate in G_{H_2}. In view of the above, a value of 0.60 was selected for G_{H_2} in agreement with Hart,[3] Allen,[5] and Barr and Schuler,[17] for the calculation of water decomposition yields given in Table X. The most reliable calculated yield, from this study, is the radical yield, G_H, which exhibits the expected trend with LET variation and is in good agreement with data of other investigators.[3,5]

Decomposition of Water. The observable water decomposition yield, G_{-H_2O}, (see equation (7) is arrived at from the stoichiometry of postulated radical-radical interactions along the track of the ionizing particle, (equations (10-12).

(10) $H + H \rightarrow H_2$

(11) $OH + OH \rightarrow H_2O_2$

(12) $H + OH \rightarrow H_2O$

The contribution of $G_{H_2SO_5}$ to the above stoichiometry is negligible (compare Tables VIII and IX) and can be neglected.

In the absence of direct experimental evidence, it is assumed[3] that reaction (12) is as probable as reactions (10) + (11).

Table X. Calculated Water Decomposition Yields and Fraction of Radicals Combining with Solute Assuming a G_{H_2} Value of 0.60.

E_P (Mev)	G_{H_2}	G_{-H_2O}[a]	G_{HOH}[b]	$G_{-H_2O(T)}$[c]	X[d]
22.0	0.60	4.17	1.45	5.62	.43
20.0	0.60	4.12	1.44	5.56	.43
18.0	0.60	4.06	1.44	5.50	.42
16.0	0.60	3.99	1.45	5.44	.41
14.0	0.60	3.92	1.45	5.37	$.40_5$
12.0	0.60	3.88	1.43	5.31	.40
10.5	0.60	3.82	1.44	5.26	.39

[a] Calculated from equation (7), $G_H + 2G_{H_2}$.

[b] Yield of water formed from recombination of H and OH.

[c] Sum of columns 3 and 4.

[d] X equals the fraction of radicals combining with solute or $G_H + G_{OH}/2G_{-H_2O(T)}$.

Therefore G_{HOH} (the reformation of water in the spur) can be calculated from equation (45), and the total yield of water decomposition is

$$(45)\quad G_{HOH} = G_{H_2} + G_{H_2O_2}$$

given by equation (46). The calculated value of G_{-H_2O} (3.82) for

$$(46)\quad G_{-H_2O(T)} = G_{-H_2O} + G_{HOH}$$

10.5 Mev protons (Table X) agrees very well with the value 3.81 reported by Barr and Schuler[17] for 18 Mev deuterons. Water decomposition values listed in Tables VIII and IX are assumed to be in error because of the large error in G_{H_2}. This factor has been considered in the tabulation of Table X. The only data available for comparing $G_{-H_2O(T)}$ values for acidified solutions are calculations of Barr and Schuler's[54] data made by Hart.[3] These calculations indicate fair agreement between the $G_{-H_2O(T)}$ value for 10.5 Mev protons (Table X) and the value calculated by Hart for 18 Mev deuterons which is 5.55 ± 0.14.

Suggestions for Further Work. The present work is extendable by use of radiations of LET in the region 0.02 to 0.2 ev/Å, for which very little experimental data exists. The impending availability of cyclotrons which can produce protons with energies up to 75 Mev (LET = 0.07 ev/Å, suggest the possibility of such an extension in the near future. Most cyclotrons in existence operate at a fixed frequency, providing a monoenergetic beam. Machines, now under construction will be capable of producing a proton beam of variable

energy. Such machines will provide the radiation chemist with a radiation source of unprecedented flexibility. The accurate determination of dosimetry, which is possible with protons and other heavy particles, will permit the much-needed resolution of discrepancies in the literature,(e.g., proposed maximum in the cerous ion yields) as well as the examination of the LET range 0.02 to 0.2 ev/Å.

Specifically, future work with cyclotron-produced radiations might improve upon or verify the present work by measurement of $G(H_2O_2)$ yields in aqueous halide solutions, and by measuring $G(H_2)$ yields using irradiation cells which are suitable for gas analysis. Other work might also examine the effect of temperature, pH, phase and scavenger concentration on the molecular and free radical yields.

VI. CONCLUSIONS

Molecular product, free radical and water decomposition yields have been determined with cyclotron-produced 11 to 23 Mev protons using ferrous sulfate, ceric sulfate and ceric + thallous sulfate dosimeters.

Over the range of LET covered in this work (0.2 to 0.4 ev/Å), experimentally determined values for $G(Fe^{+3})$ and $G(Ce^{+3})_{Tl^+}$ decreased with increasing LET, while $G(Ce^{+3})$ yields were constant. The $G(Fe^{+3})$ yields decreased from 12.8 for 23 Mev protons to 11.3 for 11 Mev protons, while $G(Ce^{+3})_{Tl^+}$ decreased from 6.78 for 23 Mev protons to 6.01 for 11 Mev protons. The $G(Ce^{+3})$ yields remained constant at 2.95 over this range of proton energy.

Calculated molecular yields G_{H_2} and $G_{H_2O_2}$ remained virtually constant over this narrow range of LET, while the free radical yields G_{OH} and G_H, and the observable yield of water decomposition G_{-H_2O}, decreased with increasing LET. The total yield of water decomposition, $G_{-H_2O(T)}$, which was calculated by assuming $G_{-H_2O(T)} = G_{-H_2O} + G_{H_2} + G_{H_2O_2}$, decreased from 4.96 for 22 Mev protons to 4.57 for 10.5 Mev protons.

The results were compared with those of other investigators. The generally good agreement with the ferric ion yield data of Hart and Anderson,[3] and the 6% disagreement of $G(Fe^{+3})$, $G(Ce^{+3})$ and $G(Ce^{+3})_{Tl^+}$ yields with the data of Schuler and Allen[2] and Barr and Schuler[17] was noted. The maximum in the cerous ion yields, suggested by Hardwick,[53] was not observed in the LET range investigated in this work.

Values and trends of the data included in this report are in qualitative agreement with the diffusion kinetics model. Direct quantitative comparison with the model was not made because of the unavailability of a computer which would permit an extension of the Ganguly and Magee[63] calculations, and because of the lack of information concerning various parameters which are required for the solution of the pertinent equations which have been derived from the diffusion kinetics theory. The data extrapolate smoothly to those obtained by Hart and Anderson,[3] which have been shown to be in accord with the one-radical diffusion model.

The work entailed accurate proton beam current and energy measurement for which methods were devised. Precise current measurement was attained by first obtaining, in a calibration procedure, a ratio of counts recorded for beam scattered to a scintillation counter by a very thin nickel foil, to the measured beam current transmitted by the foil to a Faraday cup. For irradiation of samples, the Faraday cup was replaced by the irradiation cell. From the scintillation counts recorded, and with the application of the calibration ratio, the current absorbed by the sample during irradiation was calculated.

Proton beam energies were determined from the mean range of protons in aluminum using standard range-energy relationships. Protons were degraded to approximately 6 Mev. The total range of the base beam energy was obtained from the amount of ferrous ion oxidation in a ferrous sulfate dosimeter affected by the degraded proton beam and from the amount of aluminum absorber used to degrade to beam. The method is similar to that of Schuler and

Allen,[8] but involves a more precise determination of the residual range of the degraded beam.

VII. BIBLIOGRAPHY

1. J. W. Boyle, Rad. Res., ____, (to be published), (two papers) (1962).

2. R. H. Schuler, and A. O. Allen, J. Am. Chem. Soc., 79, 1565 (1957).

3. A. R. Anderson, and E. J. Hart, Rad. Res., 14, 689 (1961).

4. C. B. Fulmer: Private communication to A. Timnick, Oak Ridge National Laboratory, Oak Ridge, Tennessee, March 11, 1958.

5. A. O. Allen, The Radiation Chemistry of Water and Aqueous Solutions, D. Van Nostrand Co., Inc., Princeton, New Jersey (1961).

6. J. Saldick, and A. O. Allen, J. Chem. Phys., 22, 438 (1954).

7. ibid., p. 1777.

8. R. H. Schuler, and A. O. Allen, Rev. Sci. Instr., 26, 1128 (1955).

9. R. H. Schuler, and A. O. Allen, J. Chem. Phys., 24, 56 (1956).

10. E. J. Hart, W. J. Ramler, and S. R. Rocklin, Rad. Res., 4, 378 (1956).

11. H. A. Schwarz, J. M. Caffrey, and G. Scholes, J. Am. Chem. Soc., 81, 1801 (1957).

12. N. Miller, and J. Wilkinson, Trans. Faraday Soc., 50, 690-710 (1954).

13. T. J. Sworski, Rad. Res., 4, 483 (1956).

14. H. A. Mahlman and J. W. Boyle: Private communication, Oak Ridge National Laboratory, Oak Ridge, Tennessee, May 8, 1962.

15. J. H. Smith, Phys. Rev., 71, 32 (1947).

16. C. M. Henderson, and N. Miller, Rad. Res., 13, 641 (1960).

17. N. F. Barr, and R. H. Schuler, J. Phys. Chem., 63, 808 (1959).

18. C. J. Hochanadel, Comparative Effects of Radiation, Ed. by M. Burton, J. S. Kirby-Smith, and J. L. Magee, Wiley and Sons, New York (1960).

19. F. S. Dainton, Rad. Res., Suppl. 1, 1 (1959).

20. E. Collinson, F. S. Dainton, and J. Kroh, Proc. Roy. Soc. (London), 265A, 422 (1962).

21. M. Burton, Ann. Rev. Phys. Chem., 1, 113 (1950).

22. F. S. Dainton, and E. Collinson, Ann. Rev. Phys. Chem., 2, 99 (1951).

23. A. O. Allen, Ann. Rev. Phys. Chem., 3, 57 (1952).

24. J. Weiss, Ann. Rev. Phys. Chem., 4, 143 (1953).

25. J. L. Magee, Ann. Rev. Nuclear Sci., 3, 171 (1953).

26. A. O. Allen, Rad. Res., 1, 85 (1954).

27. H. A. Dewhurst, A. H. Samuel, and J. L. Magee, Rad. Res., 1, 62 (1954).

28. E. J. Hart, Ann. Rev. Phys. Chem., 5, 139 (1954).

29. M. Lefort, Actions Chimique et Biologiques des Radiations, Vol. 1, Ed. by; M. Haissinsky, Masson et cie., p. 93 (1955).

30. F. S. Dainton, Ann. Rev. Nuclear Sci., 5, 213 (1955).

31. J. E. Willard, Ann. Rev. Phys. Chem., 6, 141 (1955).

32. C. J. Hochanadel, and S. C. Lind, Ann. Rev. Phys. Chem., 7, 83 (1956).

33. W. M. Garrison, Ann. Rev. Phys. Chem., 8, 129 (1957).

34. N. Miller, Rev. Pure and Appl. Chem., (Australia), 7, 123 (1957).

35. E. J. Hart, J. Chem. Ed., 29, 5 (1957).

36. E. J. Hart, Proceedings of the Second United Nations International Conference on the Peaceful Uses of Atomic Energy, 29, 5 (1958).

37. M. Lefort, Ann. Rev. Phys. Chem., 9, 123 (1958).

38. F. S. Dainton, Brit. J. Radiology, 31, 645 (1958).

39. E. J. Hart, J. Chem. Ed., 36, 266 (1959).

40. A. Charlesby, and A. J. Swallow, Ann. Rev. Phys. Chem., 10, 289 (1959).

41. W. H. Hamill, Ann. Rev. Phys. Chem., 11, 87 (1960).

42. J. L. Magee, Ann. Rev. Phys. Chem., 12, 389 (1961).

43. E. J. Hart, and R. L. Platzman, Mechanisms in Radiobiology, Vol. 1, Chapter 2, Academic Press, Inc.

44. L. H. Piette, R. C. Rempel, and H. E. Weaver, J. Chem. Phys., 30, 1623 (1959).

45. O. Oldenberg, and H. A. Frost, J. Chem. Phys., 4, 642 (1936).

46. G. von Bunau, K. C. Kurien, W. H. Taylor, and L. M. Theard, Eds., Summary of the Proceedings of an Informal Discussion of the Radiation Chemistry of Water, University of Notre Dame, (1959).

47. J. L. Magee, Basic Mechanisms in Radiobiology, Nuclear Radiation Council Publication, 305, p. 51, Washington, D. C., (1953).

48. R. L. Platzman, Basic Mechanisms in Radiobiology, Nuclear Radiation Council Publication, 305, p. 22, Washington, D. C., (1953).

49. H. A. Bethe, and J. Ashkin, Experimental Nuclear Physics, Ed. by; E. Segre, Vol. I, John Wiley and Sons, New York, N. Y. (1953).

50. E. J. Hart, W. R. McDonnell, and S. Gordon, Proceedings of the International Conference on Peaceful Uses of Atomic Energy, 7, 593 (1956).

51. A. O. Allen, and H. A. Schwarz, Proceedings of the International Conference on Peaceful Uses of Atomic Energy, 29, 30 (1958).

52. T. J. Sworski, Rad. Res., 4, 483 (1956).

53. T. J. Hardwick, Discussions Farad. Soc., 12, 303 (1952).

54. N. F. Barr, and R. H. Schuler, Rad. Res., 7, 302 (1957).

55. A. H. Samuel, and J. L. Magee, J. Chem. Phys., 21, 1080 (1953).

56. D. E. Lea, Actions of Radiations on Living Cells, Cambridge University Press, Cambridge, England (1946).

57. G. Jaffe, Ann. Physik, 42, 303 (1913).

58. G. Jaffe, Phys. Zeit., 30, 849 (1929).

59. D. E. Lea, Proc. Cambridge Phil. Soc., 30, 80 (1934).

60. E. Kara-Michailova, D. E. Lea, Proc. Cambridge Phil. Soc., 36, 101 (1940).

61. D. E. Lea, Brit. J. Radiol., Suppl. 1, 59 (1947).

62. J. L. Magee, J. Am. Chem. Soc., 73, 3270 (1951).

63. A. K. Ganguly, and J. L. Magee, J. Chem. Phys., 25, 129 (1956).

64. A. Kuppermann, Actions Chimiques et Biologiques des Radiation, Vol. 5, Ed. by M. Haissinsky, Massen et cie., (1961).

65. J. B. Ball, and C. B. Fulmer: Private communication, Oak Ridge National Laboratory, Oak Ridge, Tennessee, June 19, 1962.

66. C. B. Fulmer: Private communication, Oak Ridge National Laboratory, Oak Ridge, Tennessee, March, 1961.